Transmission from sink to patient: an evaluation of sink generated bioaerosols and their role in hospital acquired bacterial infections

JoHannah Buehrer,[a] Megan Lott,[a] Kevin Zhu,[a] Kayla Fericy,[b] Joshua Granek,[c] Claudia Gunsch,[b] A-Andrew Jones,[b] Joe Brown,[a]* Glenn Morrison,[a]* Barbara J. Turpin[a]*

a. CB #7400, Department of Environmental Sciences and Engineering, Gillings School of Global Public Health, University of North Carolina, Chapel Hill, NC 27599-7400 USA
b. CB #90287, Department of Civil and Environmental Engineering, Pratt School of Engineering, Duke University, Durham, NC 27708
c. CB #2721, Department of Biostatistics and Bioinformatics, School of Medicine, Duke University, Durham, NC 27710

*Co-corresponding authors: Joe Brown (joebrown@unc.edu), Glenn Morrison (glennmor@email.unc.edu), Barbara Turpin (bjturpin@email.unc.edu)

For submission to Journal of Aerosol Science

Abstract

Healthcare Associated Infections (HAIs) pose a significant public health risk. Hospital sinks and associated plumbing are one likely source. This study investigates bioaerosol emissions from sink P-traps during faucet operation to assess their potential role in pathogen transmission in the hospital context. We designed an aerosol chamber system with adjustable air change rate and a functioning sink meeting hospital standards. We quantified bioaerosol and large droplet emission factors from the sink, using F_{Amp} *Escherichia coli* as a model for Enterobacteriaceae such as *Klebsiella pneumoniae*. We cultured Andersen Cascade Impactor and BioSpot sampler aerosol samples and deposition plates using MI agar, which is selective for *E. coli*. Across five experiments, deposition plate counts were substantial, while air samples were close to detection limits. We estimated $PM_{5.0}$ bioaerosol emissions factors of 1.3×10^{-10} to 1.9×10^{-10} CFU emitted per CFU in P-trap. Large droplet emission factor was one order of magnitude larger, at $4.3 \times 10^{-9} \pm 2.8 \times 10^{-9}$ CFU per CFU. Results were used to predict *Klebsiella pneumoniae* inhalation dose (0.78 to 1.12 CFU day^{-1}) and inhalation infection probability (~10^{-5}) for 5.5 day hospital stay with colonized plumbing (air change rate 6 h^{-1}). This translates to ~1 infection per year for a hospital with a severe plumbing system colonization affecting ~2000 continuously occupied rooms. For pathogens with different dose response curves, we demonstrate how infection probability via inhalation depends on dose response.

Keywords: bioaerosol, hospital acquired infections, *Klebsiella pneumoniae,* microbial colonization, plumbing, P-trap

Highlights:

- Bioaerosol and droplet emission factors measured from hospital sink P-trap
- Large droplet emission factor (EF) one order of magnitude large than aerosol EF
- Patient inhalation dose and risk estimated for *K. pneumoniae* P-trap colonization
- *K. pneumoniae* infection probability via inhalation for 5.5 day stay ~10^{-5} or less
- We demonstrate application to pathogens with different dose response curves

Graphical Abstract

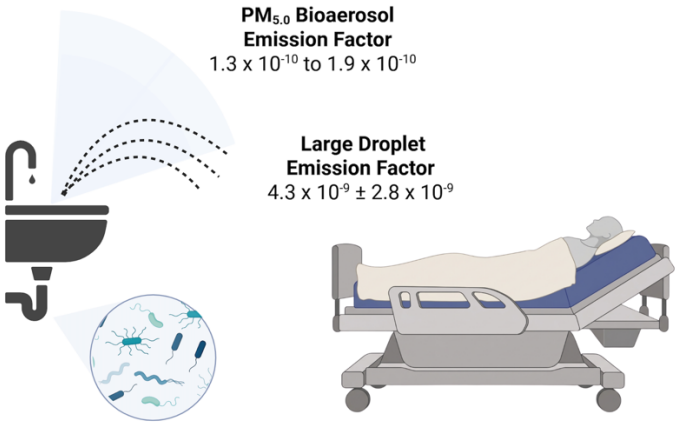

Introduction

Healthcare Associated Infections (HAIs), infections acquired while patients are receiving treatment, are among the leading causes of morbidity and mortality within the United States (U.S.; Abban et al., 2023; McFee, 2009; Monegro et al., 2025). In 2015, one out of 31 U.S. patients at any given time had a HAI, amounting to 2 million infections and an estimated 18 - 45 billion dollars in excess health care costs per year (Stone, 2009). Over 25% of HAIs are caused by antibiotic-resistant bacteria (Lerminiaux & Cameron, 2019; McFee, 2009). These bacterial infections have a high mortality rate (Abban et al., 2023). They are particularly prevalent in high-risk areas like intensive care units (ICUs) where patients are often immunocompromised (Rello et al., 2016). The prevalence of HAIs varies globally, with incidence rates in high-income countries ranging from 3.5% to 12% (Abban et al., 2023). Pneumonia is reported to account for 11% of HAIs (McFee, 2009). Elucidating the origins and transmission pathways of pathogenic organisms is a central focus of infection control research.

Mounting evidence suggests that hospital sink drains are a reservoir for pathogens in hospitals (Laço et al. 2025, McCallum & Hall 2025). Epidemiologically important pathogens, such as *Pseudomonas* spp. and *Acinetobacter* spp. and emerging antimicrobial resistant (AMR) pathogens, such as extended-spectrum β-lactamase (ESBL) and Carbapenemase-producing Enterobacterales (CPE), have been isolated from hospital sinks (Gordon et al. 2017, Wei et al. 2024, De Geyter et al. 2017, Constantinides et al. 2020). The P-trap, the curved pipe under the sink, provides a prime environment for bacterial colonization and biofilm formation due to its piping material, constant moisture, nutrient availability, and because it is uninterrupted for long periods of time (Parkes & Hota, 2018). During handwashing and sink use, the P-trap can be seeded with external bacteria, antimicrobials, and soaps which encourage the proliferation of

antimicrobial-resistant organisms (Warren et al. 2021, Kotay et al., 2019; Parkes & Hota, 2018). Bacteria present in the P-trap of one room can colonize to the P-traps of other rooms through the growth of biofilms in connected piping (Kotay et al., 2017; Volling et al., 2021).

Pathogens found in sink drains have been directly linked to patient infections (Snitkin et al. 2012, Leitner et al. 2015, Nakamura et al. 2021). Genomic analysis, epidemiological investigations, and spatial and temporal co-occurrence have matched bacterial strains between contaminated sink drainage systems and infected patients (Anantharajah et al., 2024; Tsukada et al., 2024, Volling et al., 2021). For example, in 2011, an outbreak of carbapenem-resistant *Klebsiella pneumoniae* at the U.S. National Institutes of Health (NIH) Clinical Center was linked to the patients' sink drains through genomic and epidemiological analysis (Snitkin et al. 2012). An outbreak of metallo-β-lactamase-producing *Klebsiella pneumoniae* was tied to sink traps in a New Delhi surgical intensive care unit, and the outbreak ended after replacement of the sink traps (Bourigault et al., 2025). Although the association between contaminated sinks and patient infections is well established, the specific transmission pathways remain poorly understood.

Volling et al. presented several potential transmission routes from P-trap to patient in their review of sink-related bacterial outbreaks (Volling et al., 2021). First, patients may be exposed via direct contact with sinks (Volling et al., 2021). Biofilms originating in P-traps can grow rapidly under the right conditions and eventually reach the sink strainer, and even the sink bowl (Kotay et al., 2017). Hence, bacteria could be transferred from sink surfaces to the patient or a healthcare worker's hands, and subsequently transmitted to the patient's mouth, eyes, or open wounds via touch (Volling et al., 2021). Second, particles (i.e. bioaerosols) or droplets may deposit onto nearby surfaces, fomites, or healthcare workers and be transmitted to patients through contact (Volling et al., 2021). Finally, bioaerosols generated during sink operation may

carry bacteria from the P-trap to the patient leading to exposure by direct inhalation (Volling et al., 2021).

Among the potential transmission routes discussed, the inhalation of bioaerosols generated from sink drains is the least understood (Volling et al., 2021). A field study by Dieter et al. (2025) demonstrated that viable opportunistic pathogens from hospital sink drains can be dispersed as droplets and aerosols during sink use. When examined in the laboratory, Kotay et al. (2017) detected culturable *E. coli* in air samples collected immediately after faucet operation in sinks with inoculated drains, but little or no *E. coli* in air samples collected 30 min later. The authors concluded, based on the decrease in the air concentration over 30 min, that *E. coli* containing particles in air must have been large enough to deposit rapidly (i.e., the *E. coli* were in large droplets). However, it is also possible that the *E. coli* containing particles in air were small enough to remain suspended (i.e., they were aerosols) and their concentration dropped due to ventilation. The fate of particles in indoor air, including bioaerosols and droplets, is strongly affected by their size, with particles >100 μm in diameter traveling only a few meters from their source and particles < 5 μm in diameter ($PM_{5.0}$) having deposition times that are comparable to or longer than indoor residence times (Bing-Yuan et al., 2018; Katre et al., 2021; Morawska et al., 2009). The Kotay et al results are also consistent with *E. coli* in $PM_{5.0}$ aerosol, if the laboratory air change rate (ACR) was 8-9 hr^{-1}, within the range observed commonly in laboratories. (Note: the ACR for the laboratory used in their experiments was not reported).

We posit that further research in a controlled system with lower detection limits is needed to quantify emissions and gain a better understanding of the potential for infection risk via inhalation of bioaerosol generated by faucet operation.

Therefore, the goal of the research reported herein was to measure $PM_{5.0}$ bioaerosol emissions and near-source deposition of culturable bacteria in bioaerosols and large droplets generated by sink (faucet) operation after bacteria were seeded into the P-trap of a hospital-grade sink. We used an enclosed aerosol chamber with known air change rate and high efficiency bioaerosol collection devices to reduce detection limits and better constrain factors influencing bioaerosol emission. We used the resulting data to provide information relevant to inhalation dose and infection risk for *K. pneumoniae* from colonized sink drains in hospitals. We also demonstrate the use of our results to estimate inhalation risk for epidemiologically-important pathogens with different dose response curves.

Methods

Overview of experimental approach

Details of our experimental approach are provided below and in Supplemental Information (SI) Sections S1 – S4, Tables S1 – S6, and Figures S1 – S8. In summary, we conducted 5 chamber experiments where we spiked a culture solution containing ~10^{11} Colony Forming Units (CFUs) of *Escherichia coli* F_{amp} (*E. coli* F_{amp}) into the P-trap of a sink that meets hospital design specifications. The sink was located inside a ~8 m^3 well-mixed air chamber designed for this purpose (Figure 1). After a chamber air change rate of 2.01 ± 0.05 h^{-1} with HEPA-filtered inlet air had been established for 30 min (one air change), the faucet was turned on for 3 min from outside the chamber to provide a water flow of 7.4 L min^{-1} into the sink, which is within the hand hygiene specifications of < 8.3 L min^{-1} (2018 International Plumbing Code (IPC), 2018). We hypothesized that faucet use would produce both large droplets and aerosols containing culturable *E. coli* F_{amp}. Thus, in each experiment we collected 30 deposition samples

on 100 mm x 15 mm agar plates placed in enumerated locations on horizontal surfaces in the chamber, as well as bioaerosol samples (30 min collection) using a 6-stage Andersen Cascade Impactor (Thermo Fisher, model 10-800, Franklin, MA) and a BioSpot sampler (Aerosol Devices, model BSS-300p, Fort Collins, CO). We cultured all deposition and bioaerosol samples, dividing the BioSpot sample solution onto 3 agar plates and using MI Agar (BD Diagnostics Difco™ 214883) as our growth medium, as it is selective for *E. coli*. All plates were incubated at 37 ºC for 20 - 24 hours, according to MI Agar product instructions. Following the incubation period, we counted visible colonies on all plates. Additionally, we conducted one control experiment, which was identical except that we spiked tap water rather than *E. coli* F_{amp} into the P-trap. Additional chamber experiment details are provided in Section S4. The use of an enclosed chamber to isolate the source and an air change rate that was lower than typically found in hospitals reduced (improved) detection limits and facilitated measurement of bioaerosol emission factors. Finally, we applied the bioaerosol emissions factors under conditions more typical of hospital rooms to provide insights regarding the potential for patient infection via inhalation of aerosol originating from a P-trap, given that colonization had occurred.

Chamber construction and characterization

We built the aerosol chamber by constructing an external frame with dimensions 1.83 m x 1.83 m x 2.44 m (6 ft x 6 ft x 8 ft) and lining the interior with 0.051 m x 1.22 m x 2.44 m extruded polystyrene (XPS) insulation panels. The input air was provided by a 120 mm x 120 mm x 28 mm axial exhaust fan directly attached to a HEPA filter (Organic Air, 693764510108), which distributed the flow radially to facilitate chamber air mixing; the fan voltage could be varied, providing an adjustable flow rate from ~6 $m^3\ h^{-1}$ (4 volts) to 70 $m^3\ h^{-1}$ (12 volts) under chamber conditions. The fan speed could be adjusted (10-100%) from outside the chamber, and

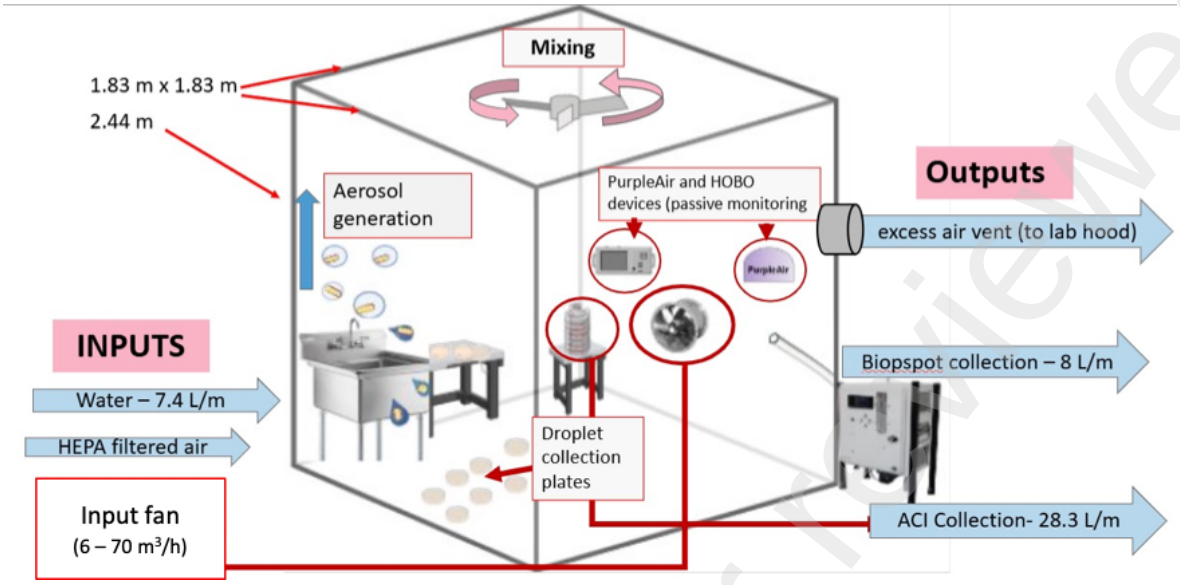

Figure 1: Air chamber (8.15 m^3) containing a functioning sink which meets hospital specifications, operated at an air change rate of 2.01 ± 0.05 h^{-1}, and instrumented with an Andersen Cascade Impactor (ACI), BioSpot sampler, deposition plates, PurpleAir particle sensor, and HOBO sensor for temperature, relative humidity and carbon dioxide measurement.

we wired a voltage reader into the power input for precise voltage readings. We placed a second fan inside the chamber mounted on the ceiling of the chamber set at 4 V (~6 m^3 h^{-1}) to provide additional internal mixing in the chamber.

We selected a sink and faucet (Table S1) based on published specifications for hospital sink designs to ensure effective hand hygiene while minimizing contamination risks in healthcare settings (2.1 North Carolina Hospitals and Outpatient Facilities Design Code 2014, 2014; Alberta Health Services, 2020). One of the key goals of the sink design requirements is to limit bacterial transmission by standardizing tap position (height from bottom of bowl and horizontal distance from drain location), drain design, and wash basin dimensions (Pirzadian et al., 2022). Water was connected from the lab to the chamber-installed sink, allowing us to turn the sink on and off without entering the chamber.

We determined the air change rate (ACR; h^{-1}) in the chamber as a function of fan voltage by injecting CO_2 into the chamber and monitoring CO_2 decay over time with a HOBO sensor (Table S2) as described in detail in Section S2. We used an ACR of 2.01 ± 0.05 h^{-1} in the five chamber experiments, which is lower than the CDC recommended value of > 5 h^{-1} in hospitals (National Institute for Occupational safety and Health, 2024) because lower ACRs result in improved, lower, detection limits for the bioaerosol emission factor.

We equipped the chamber with two bioaerosol samplers: a BioSpot sampler and an Andersen Cascade Impactor (Section S1, Table S2-S3). The BioSpot (8 L min^{-1}) is a high collection efficiency bioaerosol sampler that uses water condensation to increase the size of airborne particles, allowing the particles to be gently collected by impaction onto a liquid medium to maintain pathogen viability (BioSpot 300-P User Manual -Rev C2). We used 5 mL of collection medium, which was prepared by diluting 1M Tris-HCl (pH 8, Invitrogen™ UltraPure™) into sterile deionized water and amending the solution with HCl to a final solution of 25 mM, with a pH of 8.0 (See Section S3 Table S6 for details). Additionally, we used a 6 stage Andersen Cascade Impactor (ACI; 28.3 L/min) that collects particles between 0.65 and 7 μm in aerodynamic diameter via impaction (Table S3), providing bioaerosol size distributions. We used MI Agar (BD Difco™ 214883) prepared in glass culture plates as the 6 ACI impaction substrates. Details regarding the preparation of culture plates can be found in Section S3 – S4. Samples from both collection devices were assessed by culturing methods described below, with details in Section S3 – S4.

In addition to the bioaerosol samplers, we equipped the chamber with real-time sensors (Section S1, Table S2). We installed a PurpleAir sensor (PurpleAir Inc., Bluffdale, UT, USA), which uses light scattering to measure particle number concentration as a function of size, for

particles larger than 0.3 and smaller than 5.0 μm ($PM_{5.0}$) or 10 μm (PM_{10}) in diameter (*PurpleAir Sensors*, 2024). For these experiments we report the $PM_{5.0}$ number concentrations as supplemental information. We used a HOBO MX1102 logger to monitor temperature, CO_2 (ppm_v), and relative humidity (RH) in real time (Onset Computer Corporation, Bourne, MA, USA).

Model organism selection

We selected *E. coli* F_{amp} as a surrogate organism (see Section S3, Table S6 for details). *E. coli* F_{amp} is a lab strain that is non-infectious to humans. As a Gram-negative, non-spore forming bacilli, we propose that *E. coli* F_{amp} is suitable surrogate for other Enterobacteriaceae, such as *Klebsiella pneumoniae* (Sinclair et al., 2012).

Preparation of P-trap cultures

We prepared a stationary-phase *E. coli* F_{amp} culture in Tryptic Soy Broth (TSB) (Millipore Sigma) by incubating at 37°C for 6 h. We confirmed the concentration of the culture concentration (~10^9 CFU mL^{-1}) by spread plate or optical density at 600 nm (OD600) (See Section S4 and Table S7 for details). We seeded the P-trap with 120 mL of the bacterial culture in 30 mL increments using a sterile pipette. We placed the pipette tip through the metal strainer sink drain then slowly ejected, being careful not contaminate sink bowl or strainer with bacteria or cause splashing from P-trap.

Calculating emission factors

The bioaerosol emission factor (CFU/CFU) was calculated as the total number of CFUs of *E. coli* F_{Amp} in bioaerosol emitted from the sink divided by the number of CFUs of *E. coli* F_{Amp} spiked in the P-trap, as described in Equation 1:

$$Bioaerosol\ emission\ factor = \frac{C_a\left(\frac{CFU}{m^3}\right) * Q\left(\frac{m^3}{h}\right) * t\ (h)}{C_p\left(\frac{CFU}{mL}\right) * V\ (mL)} \quad (1)$$

where C_a is the *E. coli* F_{Amp} aerosol concentration measured by ACI or BS (CFU m^{-3}), Q is the total volumetric flow rate of air entering or leaving the chamber (16.38 $m^3\ h^{-1}$), determined from the air change rate (2.01 h^{-1}) and chamber volume (8.15 m^3), t is the sampling time (0.5 h), C_p is the concentration of *E. coli* F_{Amp} spiked into the P-trap and V is the volume spiked into the P-trap (120 mL). We assume the sink is the only source of *E. coli* F_{Amp} aerosol ($PM_{5.0}$) and that it rapidly becomes uniformly mixed in the chamber. We calculated bioaerosol emission factors for all 5 experiments, replacing values below detection limits with zero to provide a lower bound estimate and with the lower limit of detection (LLOD) to provide an upper bound estimate.

We also calculated large droplet emission factors, defined as the total number of CFUs deposited on the floor and counter in the chamber divided by the number of CFUs spiked in P-trap, described in Equation 2:

$$droplet\ emission\ factor = \frac{A_T\ (m^2) * \left(\frac{N_s\ CFU}{A_s\ m^2}\right)}{C_P\left(\frac{CFU}{mL}\right) * V\ (mL)} \quad (2)$$

where A_T is the total chamber surface area (3.34 m^2), N_s is the sum of CFUs on all 30 deposition plates, and A_s is the area of the 30 deposition plates. The 30 deposition plates covered 0.24 m^2 (A_s) of the 3.34 m^2 (A_T) available horizontal surface in the chamber. Note that many particles, even many particles larger than 5 μm, will not settle within the chamber residence time. Because of this, we note that deposition plates are likely dominated by much larger droplets. Equation 2 describes the emission factor for those large droplets.

Estimating infection probability

Using the $PM_{5.0}$ bioaerosol emissions factor derived herein, we applied a quantitative microbial risk assessment approach to estimate the probability of infection from the inhalation of bioaerosols generated from hospital P-traps contaminated with *K. pneumoniae*. *K. pneumoniae* is an opportunistic pathogen and one of the main causes of HAIs in the United States (Sitkin et al. 2011). An emerging pathogen of concern, multi-drug-resistant strains of *K. pneumoniae* are growing in prevalence and connected to hospital outbreaks from colonized sinks (Leitner et al. 2014, Constantinides et al. 2020, Nakamura et al. 2021). The transmission routes for exposure to *K. pneumoniae* from sinks remain unclear. As such, we assessed a hypothetical situation involving an occupied hospital room (floor area of 23 m^2, air volume of 57 m^3; ACR of 6 h^{-1}) where the sink drain was colonized by *K. pneumoniae* and the faucet was used once per hour.

We used a mass balance model to find the room-average concentration of *K. pneumoniae* -containing aerosol after each sink use event and the decrease in concentration with time over each hour. From these concentrations, we estimated inhaled dose, and we then applied a dose response model to predict probability of *K. pneumoniae* infection via inhalation. In this scenario, we assume the room air is well mixed. We recognize that this approach will underestimate peak exposures by someone using the sink, but we argue it provides a reasonable first level approach to assess the potential for patient exposures via aerosol transmission. Details are provided below and in SI Section S6.

The potential for *K. pneumoniae* infection via aerosol transmission in the hospital setting depends on the emission rate of infectious, inhalable particles, air change rate in the hospital room, and exposure time. For this scenario, we used the minimum ACR recommended for single hospital rooms by the World Health Organization (WHO) of 6 h^{-1} (World Health Organization,

2014). Guidelines for ICU design in the U.S. require a minimum patient room size of 23.23 m^2 (250 ft^2) (American College of Critical Care, 1995). Therefore, we considered a hospital room with an air volume (V_r) of 56.63 m^3 (250 ft^2 with 8 ft ceiling) and an ACR of 6 hr^{-1}. Bacteria concentrations in hospital P-traps are reported to range from 10^6-10^{10} CFU mL^{-1} (De Geyter et al., 2017). The concentration of *K. pneumoniae* in hospital sink P-traps is not well understood. To our knowledge there is one published study that reports *K. pneumoniae* in US hospital P-traps (Dieter et al., 2025). They concluded that *K. pneumoniae* accounted for 1% or less of bacteria across 17 rooms in one US hospital. Each room was sampled once each immediately after patient discharge. The study does not report whether any patients were infected with *K. pneumoniae* at the time of discharge. Given the uncertainty in P-trap concentrations and our interest in scenarios with *K. pneumoniae* colonization, we considered two scenarios. First, we used a *K. pneumoniae* concentration (C_p) of 1.4 x10^9 CFU mL^{-1} in a P-trap volume (V) of 120 mL, which is the average concentration spiked in the P-trap in our experiments and would suggest that at least 10% of the bacteria in the P-trap were *K. pneumoniae*. We considered this an upper bound estimate. Second, we used a P-trap concentration a factor of 10 lower, suggesting that at least 1% of the bacteria in the P-trap were *K. pneumoniae.*

We first estimated the room averaged *K. pneumoniae* concentration in aerosol as a function of time in the hospital room, assuming faucet operation once per hour over a 24 hour period. The initial concentration after 3 min of faucet operation (C_0) is given by (Equation 3):

$$C_0\left(\frac{CFU}{m^3}\right) = \frac{C_P\left(\frac{CFU}{mL}\right) * V(mL) * EF\left(\frac{CFU}{CFU}\right)}{V_r(m^3)} \quad (3)$$

where EF is the bioaerosol emission factor from Equation 1 and V_r is the volume of air in the room (56.63 m^3). After faucet use, the concentration of *K. pneumoniae* in the hospital room air

will decrease over time from its initial concentration, C_0, through exfiltration (air exchange) until the sink is used again. The bioaerosol concentration as a function of time is described by the mass balance of Equation 4 and its solution in Equation 5, assuming the only loss is exfiltration and the room is well mixed, as follows:

$$\frac{V_r dC_r}{dt} = -(\lambda)V_r C_r \quad (4)$$

$$C(t) = C_0 * e^{(-\lambda)t} \quad (5)$$

where C_r or $C(t)$ is the concentration of bacteria in room at time t (CFU m^{-3}), C_0 is the initial (peak) concentration (during sink use), λ is the air change rate (6 h^{-1}), and t is the time (h). Note: both theory and particle concentration decay experiments confirm that depositional losses of $PM_{5.0}$ are small compared to the 6 h^{-1} ACR (Section S8); therefore, we neglected depositional losses in the hospital scenario. We then estimated the inhaled dose over one hour by integrating

$$Inhaled\ dose = R_i \int_{t_1}^{t_2} C(t)dt \quad (6)$$

the predicted concentration $C(t)$ over one hour and multiplying by an adult inhalation rate (R_i) of 0.5 m^3 h^{-1} (U.S. Environmental Protection Agency, 2011), as shown in Equation 6:
Since we assume the sink and faucet are used once per hour, the 24 h dose was obtained by multiplying this hourly dose by 24, similar to the approach used by Hamilton et al (2019) for *Legionella pneumophila* in showers.

Using this inhaled dose, we estimated the probability of *K. pneumoniae* infection using the dose response model of Equation 7 and a k value of 1.62×10^{-6} based on transtracheal instillation into the lungs of rats and lobar pneumonia as the outcome (Denissen et al., 2022):

$$P_{inf,\,daily} = 1 - e^{-(dose)*k} \quad (7)$$

We calculated the probability of patient infection daily (Equation 7), over a 5.5 day hospital stay (Equation 8), and annually (Equation 8), recognizing that the annual US hospital stay is 5.5 days (2018 data; OECD, 2025):

$$P_{inf,\,n\,days} = \; 1 \; - \; (1 - \; P_{inf,\,daily})^{n} \qquad (8)$$

We assumed one faucet event occurs every hour and emits the same concentration of bacteria each time. Here, we represent the probability of infection by P_{inf}, and the inhaled dose by "*dose*". Additional details are provided in SI Section S6.

Results

Colony forming units in air samples and on deposition plates

Viable *E. coli* F_{amp} (CFU) were detected on deposition plates in all 5 experiments and in aerosol samples in 3 of 5 experiments; they were not detected in the negative control experiment

Table 1: Operating conditions and CFU of *E. coli* F_{amp} measured in aerosol and deposition samples for the 5 experiments (Exp.) and 1 dynamic blank. Samples were collected over 30 min with an Andersen Cascade Impactor (ACI) and BioSpot (BS) sampler. Experiments operated at an air change rate of 2.01 ± 0.05 h^{-1}, corresponding to an air flow rate of 16.38 ± 0.08 m^3 h^{-1}.

Experiment Name	Peak $PM_{5.0}$ concentration[a] (m^{-3})	CFU in P-trap[b]	Temperature (°C)[c]	RH (%)[c]	Total bioaerosol ACI/BS[d] (CFU)	Total Deposition[e] (CFU)
Exp. 1	3.37 x 10^4	9.0 x 10^{10}	22.6 ± 0.27	34 ± 1.1	ND/ND	38
Exp. 2	3.53 x 10^5	1.1 x 10^{11}	22.2 ± 0.01	20 ± 1.3	3/ND	74
Exp. 3	4.77 x 10^5	1.3 x 10^{11}	21.7 ± 0.00	17 ± 0.6	ND/ND	43
Exp. 4	5.90 x 10^4	4.1 x 10^{11}	22.8 ± 0.00	35 ± 1.4	2/2	70
Exp. 5	5.83 x 10^4	7.9 x 10^{10}	23.0 ± 0.30	18 ± 0.5	ND/2	13
Dynamic Blank	1.09 x 10^5	9.0 x 10^{10}	22.2 ± 0.00	16 ± 1.3	ND/ND	ND

[a]Peak $PM_{5.0}$: maximum number concentration of particles < 5 µm over the 30 min experimental run time measured by the PurpleAir Sensor (number per m^3).
[b]Total Colony Forming Units (CFU) spiked into P-trap.
[c]Temperature (°C) and relative humidity (RH): average and standard deviation across experiment.
[d]Total bioaerosol CFU measured, 30 min Andersen Cascade Impactor (ACI) and BioSpot (BS) samples post-incubation (m^3 h^{-1}).
[e]Total deposition (Dep) CFU: sum of counts from all 30 plates. Total plate area is 0.24 m^2.

(Table 1). Chamber temperature and relative humidity (RH) were 22-23 °C and 17-35% RH across experiments. All experiments were operated at a chamber ACR of 2.01 ± 0.05 h^{-1}, which corresponds to an air flow rate of 16.38 ± 0.08 m^3 h^{-1}. $PM_{5.0}$ number concentrations measured with the PurpleAir sensor are summarized in Table 1 (peak values) and shown in more detail in SI Section S7. Bioaerosol generated during sink use had a negligible impact on total $PM_{5.0}$ number concentrations, which appear to be more influenced by ambient conditions and ultrafine particles.

Bacterial colonies of *E. coli* F_{amp} were observed in ACI stages 3-6, indicating the presence of viable *E. coli* F_{amp} in aerosol particles between 0.65 μm and 4.7 μm in aerodynamic diameter (Table 2). Bioaerosol measurements were close to detection limits. A total of 3 CFU and 2 CFU of *E. coli* F_{amp} were detected in ACI samples from experiment #2 and #4, respectively, and 2 CFU and 2 CFU were detected in BioSpot samples from experiment #4 and #5, respectively (Table 2). *E. coli* F_{amp} was not detected in either ACI or BS samples collected during experiment #1 or #3. Shown in Table 2 are both counts (CFU) from bioaerosol sample substrates and air concentrations of *E. coli* F_{amp} in units of CFU m^{-3}. Given that measurements are close to LLOD, analyses below that make use of the bioaerosol concentrations have been performed using upper bound and lower bound values, i.e. for lower bound estimates we set all concentrations below LLOD equal to zero and for upper bound estimates we set all concentrations below LLOD equal to the LLOD. Using this approach, we conclude the *E. coli* F_{amp} concentration in the chamber experiments was between 2.3 and 3.9 CFU m^{-3}, averaged across all experiments (Table 2). The lower limit of detection (LLOD) for the ACI bioaerosol concentration is 1.2 CFU m^{-3}, calculated as the smallest detectable amount (1 CFU) divided by the volume of air pulled through the sampler during the 30 min collection period. For the

BioSpot, the LLOD is 4.2 CFU m^{-3}. While the higher flow rate is a big advantage for the ACI, the ACI agar impactor plates can dry out at longer sampling times. In contrast, BioSpot samples are collected into a liquid medium so that for many applications, detection limits can be reduced by simply sampling longer.

Viable *E. coli* F_{amp} were also found on the deposition plates (Figure 2). In fact, 210 CFU m^{-2} was deposited, averaged across all plates and experiments (Table 3). CFUs were found more frequently on plates placed on the counter next to the sink as shown in the heat map of Figure 2.

In fact, we observed a general trend of higher deposition frequency associated with plates that were closer to the sink (Figure 3). Sink to plate distances and deposition frequencies ranged from 39.4 cm (frequency = 5) to 130.8 cm (frequency= 1). Data are summarized in Table 3, and details can be found in Section S5 (Table S8 and S9).

Table 2: Colony forming units (CFUs) and air concentrations (CFU m^{-3}) from Biospot (BS) and Andersen cascade impactor (ACI) samples collected during 30 min chamber experiments. Values from each ACI impactor stage, as well as the sum across stages are shown, with the particle size cuts for each stage. The last column provides the average across the 5 chamber experiments, excluding the dynamic blank. ND means not detected. The LLOD for the ACI bacterial concentration is 1.2 CFU m^{-3}, and the LLOD for the BS is 4.2 CFU m^3. We provide upper bound and lower bound values for the average across the BS and ACI concentrations by setting ND = LLOD (upper bound) and by setting ND = 0 (lower bound).

	Exp. 1	Exp. 2	Exp. 3	Exp. 4	Exp. 5	Dynamic blank		
ACI CFUs	**CFU**	**CFU**	**CFU**	**CFU**	**CFU**	**CFU**	**Avg**	**Particle Diameter** (μm)
Stage 1	ND	ND	ND	ND	ND	ND		> 7
2	ND	ND	ND	ND	ND	ND		4.7 to 7.0
3	ND	1	ND	ND	ND	ND		3.3 to 4.7
4	ND	ND	ND	ND	ND	ND		2.1 to 3.3
5	ND	1	ND	ND	ND	ND		1.1 to 2.1
6	ND	1	ND	2	ND	ND		0.65 to 1.1
Sum	**ND**	**3**	**ND**	**2**	**ND**	**ND**		0.65 to >7
ACI Bacterial concentration (CFU m^{-3})	**< 1.2**	**3.5**	**< 1.2**	**2.4**	**< 1.2**	**< 1.2**		
Biospot CFUs	ND	ND	ND	2	2	ND		
BioSpot Bacterial concentration (CFU m^{-3})	**< 4.2**	**< 4.2**	**< 4.2**	**8.3**	**8.3**	**< 4.2**		
Upper bound average air concentration (CFU m^{-3}) ND = LLOD	**2.7**	**3.9**	**2.7**	**5.4**	**4.8**	**2.7**	**3.9**	
Lower bound average air concentration (CFU m^{-3}) ND = 0	**0**	**1.8**	**0**	**5.4**	**4.2**	**0**	**2.3**	

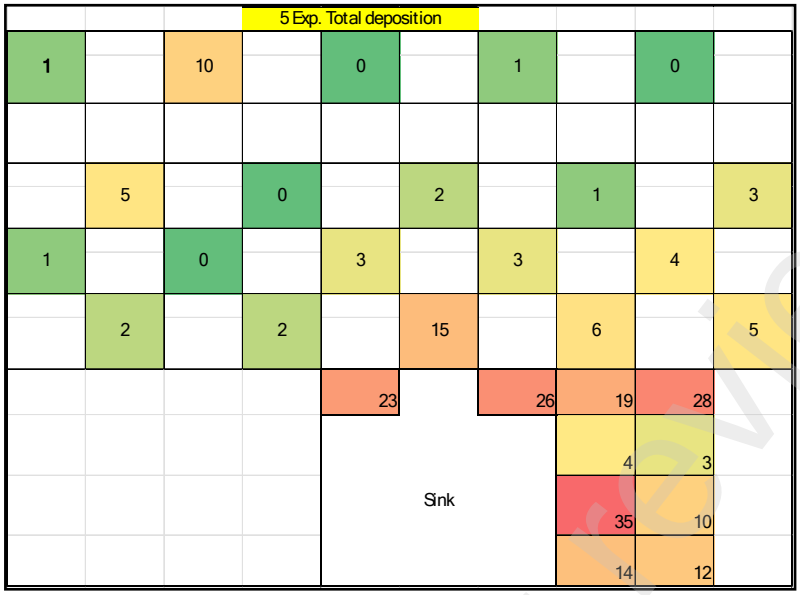

Figure 2: CFU "heat map" displaying total CFUs collected at each location, summed across experiments (N=5).

Table 3: Total CFU counted on deposition plates for each experiment and the associated surface area concentration (CFU m^{-2}).

Experiment Number	Total CFU deposition on plates	Plate surface area concentration (CFU m^{-2})	Estimated CFU deposition on entire chamber
1	38	160	540
2	77	330	1100
3	43	180	612
4	74	320	1100
5	15	64	214
Average	49	210	702
Blank	ND	< 4.3	< 14

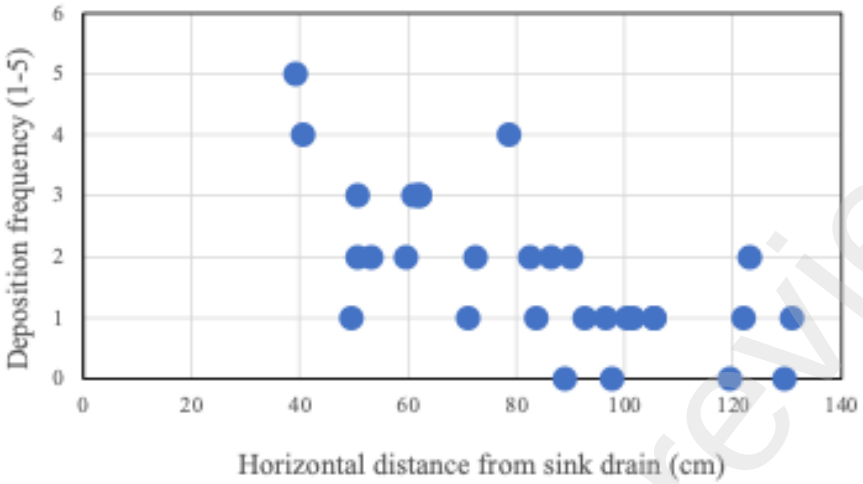

Figure 3: Frequency of *E. coli* F_{amp} presence across experiments and horizontal distance from sink drain for each counter or floor grid location. Deposition frequency ranges from 1-5 (N=5) and describes the number of experiments for which a particular location had at least one CFU.

Bioaerosol and large droplet emission factors

Bioaerosol and large droplet emissions factors are provided in Tables 4 and 5, respectively. Large droplet emission factors ($4.30 \times 10^{-9} \pm 2.81 \times 10^{-9}$), which are based on deposition data, are an order of magnitude larger than bioaerosol emission factors, which had lower and upper bound values of 1.3×10^{-10} and 1.9×10^{-10}, respectively.

Considering* K. pneumoniae *infection risk via aerosol transmission from hospital sink P-trap

Using our upper bound estimate for the concentration of *K. pneumoniae* in the P-trap (1.4×10^{9} CFU mL^{-1}), we estimated an inhalation infection risk of 6.9×10^{-6} to 1.0×10^{-5} for a patient in a room with a colonized P-trap and the average 5.5 day hospital stay; the range is obtained by applying the lower bound and upper bound bioaerosol emission factors, respectively (Table 4).

Table 4: Bioaerosol emission factors for *E. coli* F_{amp} from a hospital sink (upper and lower bounds). Shown are *E. coli* F_{amp} concentration spiked in P-trap (CFU mL^{-1}), upper and lower bound bioaerosol concentrations (CFU m^{-3}) and upper and lower bound emission factors (CFU emitted/CFU in P-trap) for each experiment (Exp).

Exp. Number	CFU in P-trap (CFU mL^{-1})	Upper bound air concentration (CFU m^{-3})	Lower bound air concentration (CFU m^{-3})	Upper bound bioaerosol emission factor (CFU/CFU)	Lower bound bioaerosol emission factor (CFU/CFU)
1	7.5×10^{8}	2.7	0	2.4×10^{-10}	0
2	8.9×10^{8}	3.9	1.8	2.9×10^{-10}	1.3×10^{-10}
3	1.1×10^{9}	2.7	0	1.7×10^{-10}	0
4	3.4×10^{9}	5.4	5.4	1.1×10^{-10}	1.6×10^{-10}
5	6.6×10^{8}	4.8	4.2	4.9×10^{-10}	3.4×10^{-10}
Average	**1.4×10^{9}**	**3.9**	**2.3**	**1.9×10^{-10}**	**1.3×10^{-10}**
Std Dev.	**1.0×10^{9}**	**1.1**	**2.2**	**1.3×10^{-10}**	**1.3×10^{-10}**

Table 5: Large droplet emission factors for *E. coli* F_{amp} from a hospital sink. Shown are *E. coli* F_{amp} concentration spiked in P-trap (CFU mL^{-1}), deposition plate concentrations (CFU m^{-3}) and emission factors (CFU emitted/CFU in P-trap) for each experiment (Exp).

Exp. Number	CFU in P-trap (CFU mL^{-1})	Plate surface area conc. (CFU m^{-2})	Large droplet emission factor (CFU/CFU)
1	7.5×10^{8}	162	6.01×10^{-9}
2	8.9×10^{8}	328	1.02×10^{-8}
3	1.1×10^{9}	183	4.79×10^{-9}
4	3.4×10^{9}	315	2.56×10^{-9}
5	6.6×10^{8}	64	2.68×10^{-9}
Average	**1.4×10^{9}**	**210**	**4.30×10^{-9}**
Std dev	**1.0×10^{9}**	**99**	**2.81×10^{-9}**

Specifically, the lower bound and upper bound bioaerosol emission factors (1.3×10^{-10} CFU/CFU and 1.9×10^{-10} CFU/CFU, respectively; Table 4) yield initial average hospital room *K. pneumoniae* air concentrations of 0.39 CFU m^{-3} and 0.56 CFU m^{-3}, respectively, immediately after sink use (Equation 3), using the *E. coli* experimental results herein as a surrogate for the behavior of *K. pneumoniae*. Bioaerosol concentrations in the hospital room then decrease with time as described in Equation 5 and shown in Figure S10 due to air exchange, until the sink is

used again one hour later, resulting in a daily dose of 0.78 to 1.12 CFU day^{-1} assuming sink use occurred once per hour. Probability of infection over 24 hours is then 1.3×10^{-6} to 1.8×10^{-6} based on lower to upper bound bioaerosol EFs. The annual infection risk would be 4.6×10^{-4} to 6.6×10^{-4}, exceeding the typical EPA benchmark of one in ten thousand infections per person per year, while also recognizing that it is rare for patients to spend an entire year in the hospital. For additional context, the annual incidence of Legionnaires' disease for the general US population was ~2.5×10^{-5} in 2017-2021 (Barskey et al., 2022; CDC, 2025); approximately one third of which occur in hospitals (Benin et al., 2002). Severe, systemic plumbing system colonization affecting 2000 occupied patient rooms with sinks would be needed to yield one infection via inhalation due to the aerosolization of *K. pneumoniae* during sink operation over the course of a year. Details can be found Section S6.

If instead the concentration of *K. pneumoniae* in the P-trap is a factor of ten lower (1.4×10^{8} CFU mL^{-1}), the dose will be a factor of ten lower, and the probability of infection via inhalation over 24 hours would be 1.3×10^{-7} to 1.8×10^{-7}. This corresponds to an order of magnitude lower inhalation infection risk for a 5.5 day hospital stay (6.9×10^{-7} to 1.0×10^{-6}) and an annual risk of 4.6×10^{-5} to 6.6×10^{-5}.

Dose response data are not available for all epidemiologically important pathogens. Using the experimentally derived emission factors and predicted daily dose for the upper bound P-trap concentration (1.4×10^{9} CFU mL^{-1}) a k value on the order of 2×10^{-5} would be needed to yield a probability of infection on the order of 10^{-4} for a 5.5 day hospital stay. A p-trap concentration a factor of ten lower would yield a dose a factor of ten lower. In this case, the k value needed to yield a probability of infection on the order of 10^{-4} for a 5.5 day hospital stay would be on the order of 2×10^{-4}. We expect that the emission factors reported herein will find

additional use in future quantitative microbial risk assessment calculations, as P-trap concentration measurements expand and dose response curves for additional pathogens become available.

Discussion

In this work, we used *E. coli* as a surrogate for Gram-negative opportunistic pathogens, such as *K. pneumoniae*. We observed culturable *E. coli* F_{amp} in $PM_{5.0}$ air samples and on deposition plates when we inoculated the hospital sink p-trap with *E. coli* F_{amp} and operated the faucet inside an 8 m^3 air chamber operated at an ACR of 2.01 h^{-1}. This is consistent with the findings of Kotay et al. (2019), who observed culturable *E. coli* in air samples and on deposition plates after inoculating a sink drain and operating a faucet in a laboratory hand washing station (no ACR reported). Because they found little or no *E. coli* in air samples collected 30 min after faucet operation, Kotay et al (2019) concluded that the particles emitted during faucet operation must be large droplets that deposited rapidly. However, as can be seen in Figure S9, ventilation alone can result in substantial reductions in air concentrations of $PM_{5.0}$ over a 30 min period. In fact, we calculate that if the ACR was 8-9 h^{-1} in the laboratory where their experiments were conducted, ventilation alone could explain their findings whether the particles emitted were large droplets or fine particles (i.e., even neglecting deposition). An ACR of 8-9 h^{-1} is well within the range of typical laboratory values (American National Standards Institute, ANSI/ASSP Z9.5-2022). The collection of size resolved samples enabled us to document the emission of *E. coli* in particles smaller than 5.0 μm in diameter. This is important because particles of this size will remain suspended long enough to mix throughout a hospital room, raising the potential for inhalation exposures. Also consistent with Kotay et al. (2019), we found that the deposition of large droplets containing *E. coli* F_{amp} decreased with increasing distance from the sink.

To extend the usefulness of our work, we calculated large droplet and bioaerosol emission factors, which can be used as inputs to indoor compartment models and computational fluid dynamics models. The large droplet emission factor is an order of magnitude larger than the bioaerosol emission factor, suggesting that most of the culturable *E. coli* displaced during faucet use is found in large droplets, not bioaerosols smaller than 5.0 μm in diameter. In a hospital patient room, transmission of *K. pneumoniae, P. aeruginosa* or other Gram negative pathogens via large droplets may be mediated by fomites or touch, whereas $PM_{5.0}$ bioaerosol can transmit these pathogens through inhalation.

To illustrate the potential for infection via inhalation, we used the bioaerosol emission factor determined herein to estimate the probability of infection assuming the sink in a patient room is colonized by *K. pneumoniae*, a common causal pathogen in respiratory infections. We assumed the faucet is used once per hour and an ACR of 6 h^{-1}. For a 5.5 day patient stay, this gives us probability of infection via inhalation on the order of 10^{-5} using our upper bound P-trap concentration. (The probability drops by a factor of ten if the concentration in the P-trap is a factor of ten lower.) Systemic colonization across 2000 continuously occupied rooms would yield on the order of one infection per year via this route.

As noted above, Gram negative infections can also occur via fomites or touch. In our work, culturable *E. coli* were detected on deposition plates placed at horizontal distances as close to the sink drain as 0.61 m and as far as 1.35 m. One previous investigation of sink-related outbreaks in hospital rooms reported that sinks in ICUs were located less than one meter from patient beds, while a separate study measured a mean value of 1.5 m (De Geyter et al., 2017; Rodger et al., 2025). Although the exact distance between patient bed and the sink may vary, these measurements from previous literature suggest a potential for sink generated droplets to

deposit on not only the patient bed but also patient care or hygiene materials, such as gloves, paper towels, or IV bag. The length of survival on surfaces and fomites depends on surface material, temperature, RH, bacteria type and nutrient availability, all of which affect the likelihood of contact exposure. The survival of pathogens on hospital room surfaces influences the risk of infection through ingestion and via open wounds, catheter sites, and ventilators.

Note that the American Hospital Association reported 6,403 hospitals in 2025, with a total of 913,136 staffed beds throughout (American Hospital Association, 2025). When infection does occur, the symptomatic severity of the infection will vary person by person. *K. pneumoniae* is an opportunistic pathogen, and often in healthy individuals an infection may be asymptomatic or mild (Snitkin et al. 2012). However, in critical care, patients are often immuno-compromised, and an infection can become life threatening. Our estimated probability of infection considers the risk of infection via inhalation alone. We note that the large droplet emission factors are an order of magnitude larger than bioaerosol emission factors. While the probability of contact with or infection from large droplets is difficult to assess, we can acknowledge that the risk of infection via large droplets warrants further investigation. We also acknowledge that our bioaerosol measurements (and emission factor) are close to our detection limits. However, this work is, to our knowledge, the first to provide an estimate of bioaerosol emissions from the P-trap that can be used to model concentration, dose and infection risk via inhalation for Gram negative bacteria colonized in sinks.

Limitations

Bioaerosol concentrations measured in this study were close to MDL. While we accounted for this in our bioaerosol emission factor estimates, future work should be conducted at a lower ACR to reduce uncertainties in the resulting bioaerosol emissions factor. Our

estimates of the bioaerosol emissions factor neglect $PM_{5.0}$ wall losses in the chamber. Additionally, we recognize that the viability of *E. coli* can be variable when harvesting from the stationary phase and can be compromised during sampling (e.g., via desiccation of agar plates over time), which could contribute to variability between experiments. Both of these limitations suggest that our reported bioaerosol emissions factors are likely lower bound values. We recognize that several factors influence the emission of bioaerosol from hospital sinks. While we used a sink that met healthcare hygiene standards, we did not explore the influence of sink and faucet design, nor did we conduct experiments after establishing a biofilm in the sink drain or explore the influence of nutrients or other materials in the sink drain. These could influence particle size and microbial viability. (Note: Kotay et al (2019) reported similar results for air samples collected in experiments with fresh inoculant and those conducted after 7 days of biofilm growth.) Future experiments could investigate the influence of faucet flow rate, biofilm presence, p-trap composition, and/or investigate surrogates for other clinically-relevant pathogens.

Conclusions

We quantified the emission of viable *E. coli* in bioaerosols and droplets that result from use of a hospital sink and faucet. To our knowledge, these are the first reported emissions factors for Gram negative bacteria in bioaerosols from hospital sink and faucet operation. Their measurement was made possible through the use of an air chamber operated at 2 air changes per hour and the use of high-efficiency bioaerosol collection instruments (BS and ACI) including one that provides size resolved samples (ACI). These findings demonstrate that Gram negative bacteria seeded into plumbing fixtures can become aerosolized in particles small enough ($PM_{5.0}$) to mix with room air and transport viable bacteria throughout the room, even when water flow

and sink design meet healthcare hygiene standards. The emissions factors can be used as inputs to compartment models or computational fluid dynamics models that simulate hospital environments for prediction of exposures and infection risk. Ultimately, our findings contribute new quantitative evidence supporting the potential for infection via inhalation of bioaerosol and via touch/fomites (i.e., mediated by large droplet deposition) and suggest the importance of continued research into the full range of transmission pathways, as well as the influence of sink/faucet design, P-trap composition, the influence of biofilm development, and surrogates for other clinically-relevant pathogens.

Acknowledgements

We acknowledge helpful conversations with Drs. Deverick Anderson (Duke University), Alexander McCumber (past UNC postdoc), Jennifer Kuzma (North Carolina State University), and Qing Dai (Duke University doctoral student), as well as assistance in the laboratory by Linden Neal (UNC doctoral student).

Funding Sources

This work was supported primarily by the Engineering Research Centers Program of the National Science Foundation under NSF Cooperative Agreement No. EEC-2133504.
J. Buehrer was supported in part as an Engineering Research Center scholar and in part as a trainee of the National Institute for Occupational Safety and Health (T42-OH008673).

Author Contributions

JoHannah Buehrer: Investigation, Formal Analysis, Writing – Original draft presentation. **Megan Lott:** Formal Analysis, Writing – Reviewing and Editing. **Kevin Zhu:** Methodology. **Kayla Fericy:** Conceptualization, Writing – Reviewing and Editing; **Joshua Granek:** Conceptualization, Writing – Reviewing and Editing; **Claudia Gunsch:** Conceptualization, Writing – Reviewing and Editing, Resources, Project administration; **A-Andrew Jones**: Conceptualization, Writing – Reviewing and Editing; **Joe Brown:** Conceptualization, Methodology, Supervision, Writing – Reviewing and Editing, Resources; **Glenn Morrison:** Conceptualization, Methodology, Investigation, Formal analysis, Supervision, Writing – Reviewing and Editing, Resources; **Barbara J. Turpin:** Conceptualization, Methodology, Formal analysis, Supervision, Writing – Reviewing and Editing, Resources, Project Administration.

Supporting Information

Supporting information is available free of charge at XXX. It includes details regarding: 1) parts, materials, media, buffer products, and instrumentation used (Sections S1 and S3), 2) air change rate calculations (Section S2), 3) methods for quantifying bacterial growth (Section S3), 4) chamber experiments (Section S4), 5) additional results (Section S5), and 6) risk calculation methods and additional results (Section S6), 7) observed chamber aerosol number concentrations (Section S7), 8) additional consideration of particle losses in the chamber (Section S8), 8) associated references (Section S9).

References

Abban, M. K., Ayerakwa, E. A., Mosi, L., & Isawumi, A. (2023). The burden of hospital acquired infections and antimicrobial resistance. *Heliyon*, *9*(10), e20561. https://doi.org/10.1016/j.heliyon.2023.e20561

Alberta Health Services. (2020). *Recommendations for Hand Hygiene Sink Requirements*.

https://www.albertahealthservices.ca/assets/healthinfo/ipc/if-hp-ipc-guidelines-sink-and-faucet-selection.pdf.

American College of Critical Care. (1995). Guidelines for intensive care unit design. *Critical Care Medicine*, *23*(3), 582–588.

American Hospital Association. (2025). *Fast facts on U.S Hospitals, 2025*. American Hospital Assoiation. https://www.aha.org/statistics/fast-facts-us-hospitals

Anantharajah, A., Goormaghtigh, F., Nguvuyla Mantu, E., Güler, B., Bearzatto, B., Momal, A., Werion, A., Hantson, P., Kabamba-Mukadi, B., Van Bambeke, F., Rodriguez-Villalobos, H., & Verroken, A. (2024). Long-term intensive care unit outbreak of carbapenemase-producing organisms associated with contaminated sink drains. *Journal of Hospital Infection*, *143*, 38–47. https://doi.org/10.1016/j.jhin.2023.10.010

Barskey, A.E., Derado, G. & Edens, C. (2022). Rising incidence of Legionnaires' disease and associated epidemiologic patterns, United States, 1992–2018. *Emerging Infectious Diseases*, *28*(3), 527.

Bing-Yuan, Zhang, Y.-H., Leung, N. H. L., Cowling, B. J., & Yang, Z.-F. (2018). Role of viral bioaerosols in nosocomial infections and measures for prevention and control. *Journal of Aerosol Science*, *117*, 200–211. https://doi.org/10.1016/j.jaerosci.2017.11.011

Bourigault, C., Andreo, A., Mangeant, R., Le Gallou, F., Marquot, G., Latte, D.D.D., Mahé, P.J., Birgand, G., Bidon, C., Asehnoune, K. & Corvec, S., 2025. Hospital outbreak of NDM-producing *Klebsiella pneumoniae* in a surgical intensive care unit: Sink traps as the causing source of epidemic strain resurgence. *American Journal of Infection Control*, *53*(5), 648-651.

Constantinides B., Chau K.K., Quan T.P., Rodger G., Andersson M.I., Jeffery K., Lipworth S., Gweon H.S., Peniket A., Pike G., Millo J., Byukusenge M., Holdaway M., Gibbons C., Mathers A.J., Crook D.W., Peto T.E.A., Walker A.S., Stoesser N. (2020). Genomic surveillance of *Escherichia coli* and *Klebsiella spp.* in hospital sink drains and patients. *Microbial Genomics*, 6(7), mgen000391. doi: 10.1099/mgen.0.000391.

CDC, Legionnaires' Disease Surveillance Summary Report, United States 2020-2021. December, 2025. https://www.cdc.gov/legionella/php/surveillance/surveillance-report-2020-2021.html

De Geyter, D., Blommaert, L., Verbraeken, N., Sevenois, M., Huyghens, L., Martini, H., Covens, L., Piérard, D., & Wybo, I. (2017). The sink as a potential source of transmission of carbapenemase-producing Enterobacteriaceae in the intensive care unit. *Antimicrobial Resistance & Infection Control*, *6*(1), 24. https://doi.org/10.1186/s13756-017-0182-3

Denissen, J., Reyneke, B., Waso-Reyneke, M., Havenga, B., Barnard, T., Khan, S. & Khan, W. (2022). Prevalence of ESKAPE pathogens in the environment: Antibiotic resistance status, community-acquired infection and risk to human health. *International Journal of Hygiene and Environmental Health*, *244*, 114006.

Dieter, L., Bowie, K., Luhung, I., Healy, H. G., Roberts, S. C., Mathew, T., Peaper, D., Martinello, R. A., Gerstein, M. B. & Peccia, J. (2025). Aerosol-Based Exposure to Opportunistic Pathogens Originating from Hospital Sink Drains. *American Journal of Infection Control,* Advance on-line publication. https://doi.org/10.1016/j.ajic.2025.10.030.

Gordon, A., Mathers, A., Cheong, E., Gottlieb, T., Kotay, S., Walker, A.S. Peto, T.E.A, Crook, D.W. & Stoesser, N. (2017). The Hospital Water Environment as a Reservoir for Carbapenem-Resistant Organisms Causing Hospital-Acquired Infections—A Systematic Review of the Literature, *Clinical Infectious Diseases*, 64(10), 1435–1444, https://doi.org/10.1093/cid/cix132

Hamilton, K.A., Hamilton, M.T., Johnson, W., Jjemba, P., Bukhari, Z., LeChevallier, M., Haas, C.N. & Gurian, P.L. (2019). Risk-based critical concentrations of *Legionella pneumophila* for indoor residential water uses. *Environmental Science & Technology*, *53*(8), 4528-4541.

Katre, P., Banerjee, S., Balusamy, S., & Sahu, K. C. (2021). Fluid dynamics of respiratory droplets in the context of COVID-19: Airborne and surfaceborne transmissions. *Physics of Fluids*, *33*(8) 081302. https://doi.org/10.1063/5.0063475

Kotay, S., Chai, W., Guilford, W., Barry, K., & Mathers, A. J. (2017). Spread from the Sink to the Patient: *In Situ* Study Using Green Fluorescent Protein (GFP)-Expressing *Escherichia coli* to Model Bacterial Dispersion from Hand-Washing Sink-Trap Reservoirs. *Applied and Environmental Microbiology*, *83*(8), e03327-16. https://doi.org/10.1128/AEM.03327-16

Kotay, S. M., Donlan, R. M., Ganim, C., Barry, K., Christensen, B. E., & Mathers, A. J. (2019). Droplet- Rather than Aerosol-Mediated Dispersion Is the Primary Mechanism of Bacterial Transmission from Contaminated Hand-Washing Sink Traps. *Applied and Environmental Microbiology*, *85*(2), e01997-18. https://doi.org/10.1128/AEM.01997-18

Laço J., Martorell S., Gallegos M., Gomila M. (2025) Yearlong analysis of bacterial diversity in hospital sink drains: culturomics, antibiotic resistance and implications for infection control. *Frontiers in Microbiology,* 15, 1501170. doi: 10.3389/fmicb.2024.1501170

Leitner E., Zarfel G., Luxner J., Herzog K., Pekard-Amenitsch S., Hoenigl M., Valentin T., Feierl G., Grisold A.J., Högenauer C., Sill H., Krause R. & Zollner-Schwetz I. (2015) Contaminated handwashing sinks as the source of a clonal outbreak of KPC-2-producing *Klebsiella oxytoca* on a hematology ward. *Antimicrobial Agents and Chemotherapy*, 59(1), 714-716. doi: 10.1128/AAC.04306-14.

Lerminiaux, N. A. & Cameron, A. D. S. (2019). Horizontal transfer of antibiotic resistance genes in clinical environments. *Canadian Journal of Microbiology*, *65*(1), 34–44. https://doi.org/10.1139/cjm-2018-0275

McCallum, G.E., Hall, J.P.J. (2025) The hospital sink drain microbiome as a melting pot for AMR transmission to nosocomial pathogens. *npj Antimicrobials and Resistance,* 3, 68. https://doi.org/10.1038/s44259-025-00137-9

McFee, R. B. (2009). Nosocomial or Hospital-acquired Infections: An Overview. *Disease-a-Month*, *55*(7), 422–438. https://doi.org/10.1016/j.disamonth.2009.03.014

Monegro, A., Muppidi, V., & Regunath, H. (2025). Hospital Acquired Infections. In *StatPearls*. StatPearls Publishing. https://www.ncbi.nlm.nih.gov/books/NBK441857/

Morawska, L., Johnson, G. R., Ristovski, Z. D., Hargreaves, M., Mengersen, K., Corbett, S., Chao, C. Y. H., Li, Y., & Katoshevski, D. (2009). Size distribution and sites of origin of droplets expelled from the human respiratory tract during expiratory activities. *Journal of Aerosol Science*, *40*(3), 256–269. https://doi.org/10.1016/j.jaerosci.2008.11.002

Nakamura I, Yamaguchi T, Miura Y, Watanabe H. (2021) Transmission of extended-spectrum β-lactamase-producing *Klebsiella pneumoniae* associated with sinks in a surgical hospital ward, confirmed by single-nucleotide polymorphism analysis. *Journal of Hospital Infections*, 118:1-6. doi: 10.1016/j.jhin.2021.08.013.

North Carolina Hospitals and Outpatient Facilities Design Code 2014, 2014 Facility Guidlines Institute Code. Section 2.1 Hand-Washing Station Sinks (2014). https://fgiguidelines.org/codes/editions/

Parkes, L. O., & Hota, S. S. (2018). Sink-Related Outbreaks and Mitigation Strategies in Healthcare Facilities. *Current Infectious Disease Reports*, *20*(10), 42. https://doi.org/10.1007/s11908-018-0648-3

Pirzadian, J., Souhoka, T., Herweijer, M., Van Heel, L., Van Wamel, W. J. B., Goossens, R. H. M., Severin, J. A., & Vos, M. C. (2022). Impact of sink design on bacterial transmission from hospital sink drains to the surrounding sink environment tested using a fluorescent marker. *Journal of Hospital Infection*, *127*, 39–43. https://doi.org/10.1016/j.jhin.2022.04.017

PurpleAir Sensor. (2024, August 6). [Informational]. API-PurpleAir. https://api.purpleair.com/#api-sensors-get-sensor-data

Ramírez-Estrada, S., Borgatta, B. & Rello, J. (2016). *Pseudomonas aeruginosa* ventilator-associated pneumonia management. *Infection and Drug Resistance*, 9, 7-18. https://doi.org/10.2147/IDR.S50669

Rodger, G., Chau, K.K., Aranega Bou, P., Moore, G., Roohi, A., The SinkBug Consortium, Walker, A.S., & Stoesser, N. (2025). Survey of healthcare-associated sink infrastructure, and sink trap antibiotic residues and biochemistry, in 29 UK hospitals. *Journal of Hospital Infection*, 159, 140-147. https://doi.org/10.1016/j.jhin.2025.02.002

Sinclair, R.G., Rose, J.B., Hashsham, S.A., Gerba, C.P. & Haas, C.N. (2012). Criteria for selection of surrogates used to study the fate and control of pathogens in the environment. *Applied and Environmental Microbiology*, *78*(6), 1969-1977.

Snitkin E.S., Zelazny A.M., Thomas P.J., Stock F., NISC Comparative Sequencing Program Group, Henderson, D.K., Palmore, T.N. & Segre, J.A. (2012) Tracking a hospital outbreak of carbapenem-resistant *Klebsiella pneumoniae* with whole-genome sequencing. Science Translational Medicine, 4(148):148ra116. doi: 10.1126/scitranslmed.3004129.

Stone, P. W. (2009). Economic burden of healthcare-associated infections: An American perspective. *Expert Review of Pharmacoeconomics & Outcomes Research*, *9*(5), 417–422. https://doi.org/10.1586/erp.09.53

Tsukada, M., Miyazaki, T., Aoki, K., Yoshizawa, S., Kondo, Y., Sawa, T., Murakami, H., Sato, E., Tomida, M., Otani, M., Kumade, E., Takamori, E., Kambe, M., Ishii, Y., & Tateda, K. (2024). The outbreak of multispecies carbapenemase-producing Enterobacterales associated with pediatric ward sinks: IncM1 plasmids act as vehicles for cross-species transmission. *American Journal of Infection Control*, *52*(7), 801–806. https://doi.org/10.1016/j.ajic.2024.02.013

U.S. Environmental Protection Agency. (2011). Chapter 6: Inhalation Rates. In *Exposure Factors Handbook: 2011 Edition* (2011th ed., pp. 6–1 to 6–81). U.S. Environmental Protection Agency. https://www.epa.gov/sites/default/files/2015-09/documents/efh-chapter06.pdf

Volling, C., Ahangari, N., Bartoszko, J. J., Coleman, B. L., Garcia-Jeldes, F., Jamal, A. J., Johnstone, J., Kandel, C., Kohler, P., Maltezou, H. C., Maze Dit Mieusement, L., McKenzie, N., Mertz, D., Monod, A., Saeed, S., Shea, B., Stuart, R. L., Thomas, S., Uleryk, E., & McGeer, A. (2021). Are Sink Drainage Systems a Reservoir for Hospital-Acquired Gammaproteobacteria Colonization and Infection? A Systematic Review. *Open Forum Infectious Diseases*, *8*(2), ofaa590. https://doi.org/10.1093/ofid/ofaa590

Warren, B., Smith, B., Lewis, S., Anderson, D. & Addison, B. (2021) *Klebsiella pneumoniae* Carbapenemase (KPC)–Producing *K. pneumoniae* Contamination of an In-Room Sink in a New Bed Tower. Antimicrobial Stewardship & Healthcare Epidemiology, 1(S1):s73. doi: 10.1017/ash.2021.143. PMCID: PMC9551509.

Wei, L., Feng, Y., Lin, J., Kang, X., Zhuang, H., Wen, H., Ran, S., Zheng, L., Zhang, Y., Xiang, Q., Liu, Y., Wu, X., Duan, X., Zhang, W., Li, Q., Guo, H., Tao, C. & Qiao, F. (2024) Handwashing sinks as reservoirs of carbapenem-resistant *Acinetobacter baumannii* in the intensive care unit: a prospective multicenter study. *Frontiers in Public Health*, 12:1468521. doi: 10.3389/fpubh.2024.1468521.

World Health Organization. (2014). *Infection prevention and control of epidemic- and pandemic-prone acute respiratory infections in health care*. World Health Organization. https://iris.who.int/handle/10665/112656

Supplemental Information:

Transmission from sink to patient: an evaluation of sink generated bioaerosols and their role in hospital acquired bacterial infections

JoHannah Buehrer,[a] Megan Lott,[a] Kevin Zhu,[a] Kayla Fericy,[b] Joshua Granek,[c] Claudia Gunsch,[b] A-Andrew Jones,[b] Joe Brown,[a]* Glenn Morrison,[a]* Barbara J. Turpin[a]*

a. CB #7400, Department of Environmental Sciences and Engineering, Gillings School of Global Public Health, University of North Carolina, Chapel Hill, NC 27599-7400 USA
b. CB #90287, Department of Civil and Environmental Engineering, Pratt School of Engineering, Duke University, Durham, NC 27708
c. CB #2721, Department of Biostatistics and Bioinformatics, School of Medicine, Duke University, Durham, NC 27710

*Co-corresponding authors: Joe Brown (joebrown@unc.edu), Glenn Morrison (glennmor@email.unc.edu), Barbara Turpin (bjturpin@email.unc.edu)

Table of Contents

Section S1. Experimental Parts and Materials

Table S1: Chamber parts and materials

Part	Dimensions and details	Manufacturer information
PROFLO Lisbon Valley Vitreous China Pedestal Bathroom Sink	• Overall Height: 20.6 cm (8.125 in) from top to bottom of sink • Overall Length: 51.4 cm (20.25 in) from left to right of sink • Overall Width: 45.7 cm (18 in) from front to back of sink • Basin Length: 42.5 cm (16.75 in) from left to right of basin • Basin Width: 28.9 cm (11.375 in) from front to back of basin) • Basin Depth: 14.6 cm (5.75 in) from top to bottom of basin • Faucet Centers: 20.3 cm (8.0 in) distance between outer faucet holes • Drain Connection Size: 3.8 cm (1.5 in) • Number of Faucet Holes: 3	PROFLO, Ferguson Enterprises Model: PF5008WH Newport News, Virginia, USA
20 cm (8 in) Centerset with Exposed Deck Faucet Gooseneck Spout	L: 40.6 cm (16 in) W: 24.1 cm (9.5 in) H: 44.0 cm (17.3125 in) 10.2 cm (4 in) Wristblade Handle 20.3 cm (8 in) Spout reach	Elkay Manufacturing Company Model: LK810GN08T4 Downers Grove, Illinois, USA
Hose Vary 10 cm (4 in) Axial Exhaust Fan	12.2 cm L x 3.86 cm W x 12.2 cm H (4.8 in L x 1.52 in W x 4.8 in H) 10.2 cm (4 in) fan diameter 12 Volts 7 Watts 3000 RPM	Hose Vary Model: B0B2PBQY8W Location not provided
HEPA Filter 10 cm (4 in)	16.3 cm L x 16.0 cm W x 19.1 cm H (6.4 in L x 6.3 in W x 7.5 in H)	Organic Air Model: B0032JULB4 Location not provided
Primary calibrator 4046 (Volumetric flow meter)	Measures volumetric flow from 2.5-300 (±2%) L/m	Thermo-Systems Engineering Co. (TSI) Model: 4046 Shoreview, MN, USA

Table S2: Instrumentation and sensors used

Sampling Devices				
Instrument	**Description**	**Sample Rate**	**Manufacturer information**	**Deposition media**
BioSpot™ Bioaerosol Collector	Gently captures bioaerosols in liquid medium	8 L min^{-1}	Aerosol Devices INC. Model: BSS-300p Serial No. 1905-08B Fort Collins, CO USA	Liquid TRIS buffer solution
Andersen Cascade Impactor	Captures viable bioaerosols in sized fractions	28.3 L min^{-1}	Thermo Fisher Scientific Series 10-800 Serial No. S-0089 Franklin, MA, USA	MI agar plates
HOBO^{R} MX Co2 Logger	Measures the temperature and RH of the chamber	N/A – passive sampling	ONSET Computer Corporation. Series MX1102 Serial No. 21742231 Bourne, MA, USA	N/A
PurpleAir Air Quality Sensor	Uses laser and light scattering to capture particle size distribution	N/A- passive sampling	PurpleAir, Inc. Model BME280 Device-ID: C8:C9:A3:27:5D:66 Bluffdale, UT, USA	N/A
SmartSpec Plus spectrophotometer	Measures how much light a substance absorbs at specific wavelengths to determine its optical density	N/A	Bio-Rad Laboratories, Inc. Model: SmartSpec Plus Serial No. 273 BR 03781 Hercules, CA USA	N/A

Table S3: Andersen Cascade Impactor (ACI) impactor size cuts. D_{50} is the cutpoint diameter, the aerodynamic particle diameter for which the collection efficiency is 50%. from EPM Six Stage impactor manual (Thermo Fisher Scientific, 2009).

Stage	Particle collection range
1	particles > 7 µm (D_{50} ~7.0 µm)
2	4.7 < particles < 7.0 µm (D_{50}~ 4.7 µm)
3	3.3 < particles < 4.7 µm (D_{50} ~3.3 µm)
4	2.1 < particles <3.3 µm (D_{50} 2.1 µm)
5	1.1 < particles < 2.1 µm (D_{50} 1.1µm)
6	0.65 < particles < 1.1 (D_{50} 0.65 µm)

Section S2. Determination of Chamber Air Change Rate (ACR) as a function of fan voltage

During each ACR experiment, the fan speed was set, fan voltage recorded, and the chamber door was sealed. We first measured the baseline CO_2 concentration with the HOBO. Next, we injected CO_2 for 30 seconds. We then monitored the CO_2 decay over several hours. Once CO_2 levels approached baseline values, we stopped the experiment and downloaded data. ACR was determined using the measured CO_2 concentration and applying a mass balance (Equation S1). Note this equation assumes that CO_2 deposition is negligible.

$$\frac{dC(t)}{dt} = \lambda[C_{inlet} - C(t)] \quad \text{(S1)}$$

where $C(t)$ is the concentration of CO_2 at time t (µg m^{-3}); C_{inlet} is the concentration of CO_2 entering the chamber (µg m^{-3}), and λ is the air change rate (h^{-1}). The solution is given in Equation S2 and can be rewritten as provided in Equation S3, where C_0 is initial background CO_2 concentration (µg m^{-3}) in the chamber.

$$C(t) = C_{inlet} + (C_o - C_{inlet})e^{-\lambda t} \quad \text{(S2)}$$

$$-\ln\left(\frac{C(t) - C_{inlet}}{C_o - C_{inlet}}\right) = \lambda t \quad \text{(S3)}$$

Figure S1 provides the CO_2 concentration over time in an example ACR experiment, and the slope in Figure S2 is a visual representation of the ACR for the same experiment. Table S4 and Figure S3 summarize the results of all ACR experiments. Ultimately, we chose to set the chamber fan to 6.2 V, as it achieved the target ACR of 2 h^{-1}.

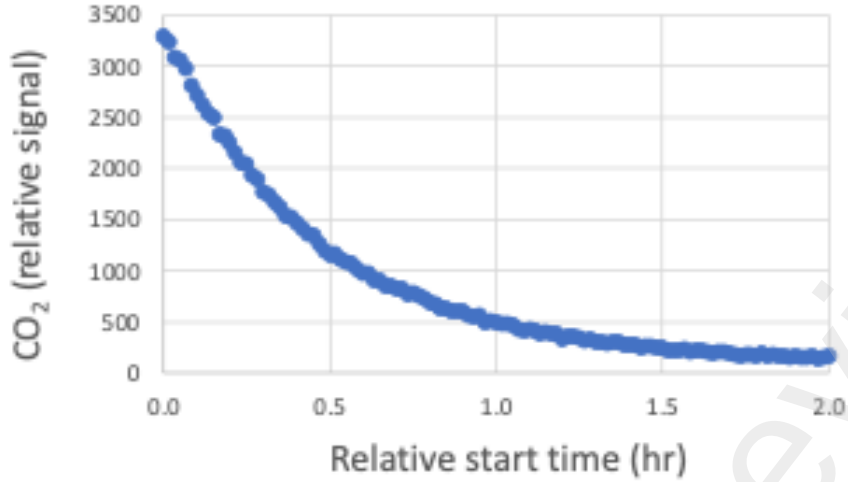

Figure S1: The decrease in CO_2 (raw signal) over the course of two hours at a fan voltage 6.19 (±0.01) V.

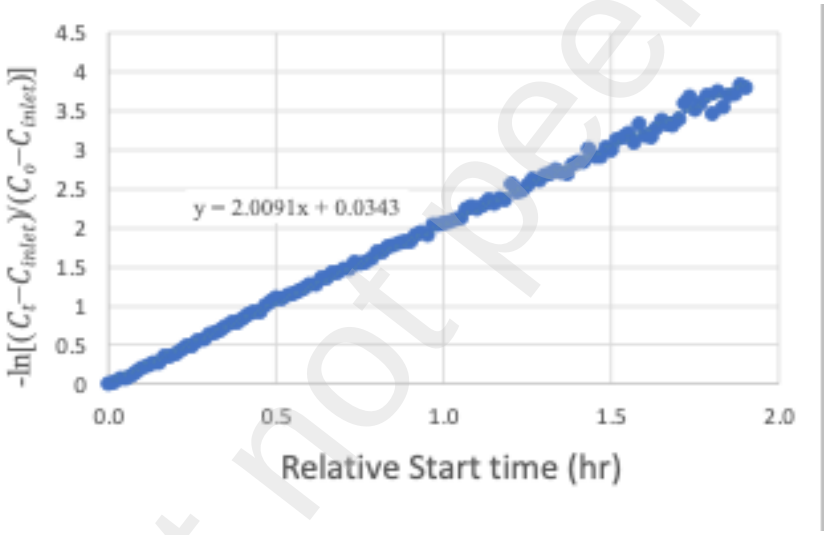

Figure S2: Slope represents the air change rate (h^{-1}) over the course of two hours with fan at 6.19 (±0.01) V.

Table S4: Summary of ACR experiments with fan voltages, air change rates (ACR) and volumetric flow rates (Q).

Experiment #	Fan voltage (V)	ACR h^{-1}	Q $m^3 h^{-1}$
1	4.31 (±0.01)	0.80	6.52
2	4.40 (±0.01)	0.87	7.09
3	5.16 (±0.01)	1.48	12.06
4	6.30 (±0.01)	2.12	17.28
5	6.19 (±0.01)	2.01	16.38
6	10.5 (±0.01)	7.42	60.47
7	12.20 (±0.01)	8.63	70.33

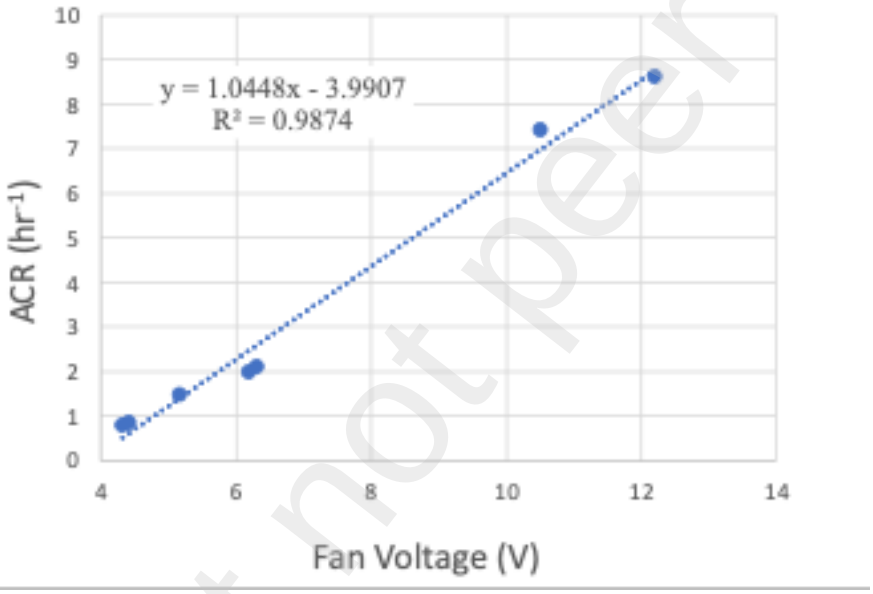

Figure S3: Fan voltage and ACR with associated linear equation and coefficient of determination (R^2)

An ACR of 2 h^{-1} was selected for bioaerosol experiments. Although this rate is lower than recommended for hospital ventilation, a lower ACR provides higher chamber air concentrations and increases the probability that we will measure a detectable emission rate. We expressed the uncertainty in the ACR as the standard error of the slope of the linear relationship

between fan voltage and ACR (Table S5). The ACR for a fan speed of 6.19 ± 0.01 V is 2.01 ± 0.05 hr^{-1}.

Table S5: The regression statistics for the relationship between fan voltage and ACR.

	Coefficients	*Standard Error*	*t Stat*	*P-value*	*Lower 95%*	*Upper 95%*	*Lower 95.0%*	*Upper 95.0%*
Intercept	-3.99073154	0.399848405	-9.98061	0.000173	-5.018574583	-2.96288849	-5.018574583	-2.96288849
Fan voltage (V)	1.044845511	0.0527857	19.7941	6.08E-06	0.909155549	1.180535472	0.909155549	1.180535472

Section S3: Quantifying bacterial growth using colony forming units (CFU), optical density (OD) and growth curves

We developed growth curves for *E. coli* F_{Amp} in batch culture and compared with OD measurements. Each bacterial growth experiment was conducted over the span of 6 hours after an initial growth period of 18 hours. To standardize the initial bacterial concentration, we grew the *E. coli* via the streak plate method, which enabled us to isolate individual colonies of the bacteria. One colony was removed with a sterile inoculation loop and swirled into 30 mL of Tryptic Soy Broth (TSB) (Table S6). This culture was placed in an incubator at 37 degrees C with shaking for 18 hours. After this initial growth period, we measured and recorded the OD at 520 nm. We continued the protocol as outlined, removing 100 µL of this culture and placing it into 30 mL of fresh TSB. To have enough volume to make serial dilutions throughout, we used 90 mL of TSB and transferred 300 µL of the culture, swirling the culture to ensure uniformity throughout. We took the optical density of this new culture and removed enough to make serial dilutions before placing it back in the incubator for 30 minutes under the same conditions. While the culture was growing, we diluted it from 10^1-10^6 using 100 µL of the culture and 900 µL of Phosphate Buffer solution (PBS) (Table S6). We placed 50 µL of the 10^4, 10^5, and 10^6 dilutions on freshly poured TSA plates (Table S6) in triplicate and set to the side. This same procedure

was repeated every 30 min for 6 hours total, generating 13 timepoints (T0-T12), one every 30 min. Starting at timepoint 7, we made additional dilutions up to 10^7 and plated 10^5-10^7 in triplicate to adjust for the increase in CFUs. After the 6 hours elapsed, all 117 plates were incubated for 12 h

Table S6: Media and buffer products used for bacterial culture and sample collection.

Materials			
Chemical	**Supplier**	**Product ID**	**Components/details**
BD Bacto Tryptic Soy Agar	Fisher Scientific	DF0369-17-6	Pancreatic digest of Casein 15 g L^{-1}, Papaic digest of Soybean 5 g L^{-1}, Sodium Chloride 5 g L^{-1}, Agar 15 g L^{-1}
BD Bacto Tryptic Soy Broth	Fisher Scientific	DF0370-17-3	Pancreatic digest of Casein 17 g L^{-1}, Papaic digest of Soybean 3 g L^{-1}, Dextrose 2.5 g L^{-1}, Sodium Chloride 5 g L^{-1}, Dipotassium Phosphate 2.5 g L^{-1}
BD Difco™ Chromogenic Dehydrated Culture Media: MI Agar	Fisher Scientific	B14883	Proteose Peptone No. 3 at 5 g L^{-1}, Yeast extract 3 g L^{-1}, D-Lactose 1 g L^{-1}, 4-Methylumbelliferyl-beta-D-galactopyranoside 0.1 g L^{-1}, Indoxyl-beta-D-glucuronide 0.32 g L^{-1}, Sodium Chloride 7.5 g L^{-1}, Dipotassium Phosphate 3.3 g L^{-1}, Monopotassium Phosphate 1 g L^{-1}, Sodium Lauryl Sulfate 0.2 g L^{-1}, Sodium Desoxycholate 0.1 g L^{-1}, Agar 15 g L^{-1}
Corning™ Cell Culture Phosphate Buffered Saline (1X)	Fisher Scientific	MT21040CV	Potassium Dihydrogen Phosphate 0.144 g L^{-1}, Sodium Chloride 9 g L^{-1}, Disodium Phosphate 0.795 g L^{-1}
Invitrogen™ UltraPure™ 1M Tris-HCI, pH 8.0	Fisher Scientific	15-568-025	For 100 mL: Tris(hydroxymethyl)aminomethane (Tris) base 12.11 g, DI water 80 mL, HCl addition until desired PH (8.0) has been reached, top with DI water until volume reaches 100 mL (Thermo Fisher Scientific, 2020)
E. coli F_{AMP}	American Type Culture Collection (ATCC)	ATCC# 700891	*E. coli* F_{AMP}— *E. coli* HS(pFamp)R (male-specific coliphage host)—originated by Victor Cabelli, formerly of the Department of Microbiology, University of Rhode Island, Kingston, RI, USA, frozen stock.

at 37 °C. After the incubation period, we counted the colonies on each dilution plate and plotted the relationships between OD and time, CFU mL^{-1} and time, and finally CFU mL^{-1} and OD. We performed the bacterial growth experiments three times using the final protocol, enabling us to quantify the *E. coli* F_{Amp} culture. Results from bacterial growth experiments are shown in Figures S4-S7. These figures show that both OD and CFU mL^{-1} increase slowly for the first ~100 min, then increase logarithmically before reaching a point of stagnation. Figure S6-S7 show the linear relationship between OD and CFU mL^{-1}, and although the values from the three experiments vary during the period of logarithmic growth, they show little variability at timepoint 12 implying the relationship between OD and CFU mL^{-1} is consistent at that time, as cultures reach their peak growth. This is highlighted as we will incubate the *E. coli* culture under the same time/heat conditions during our chamber experiments, and the P-trap cultures will be taken from timepoint 12.

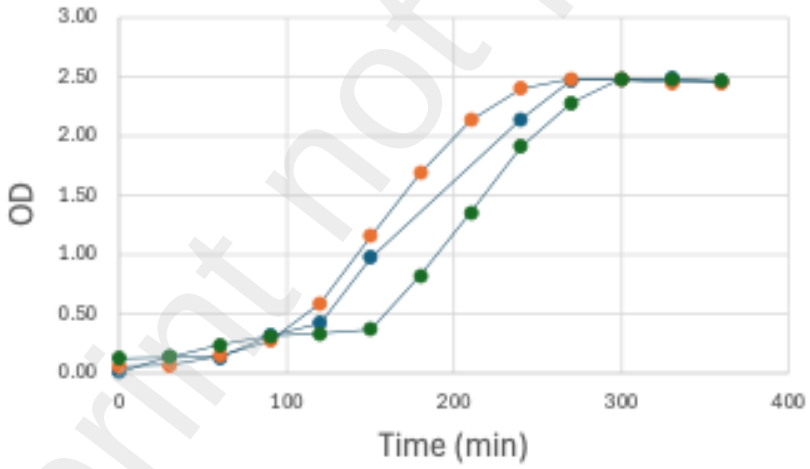

Figure S4: Optical Density (OD; wavelength=520 nm) and time (min) for bacterial growth experiments. (N=3).

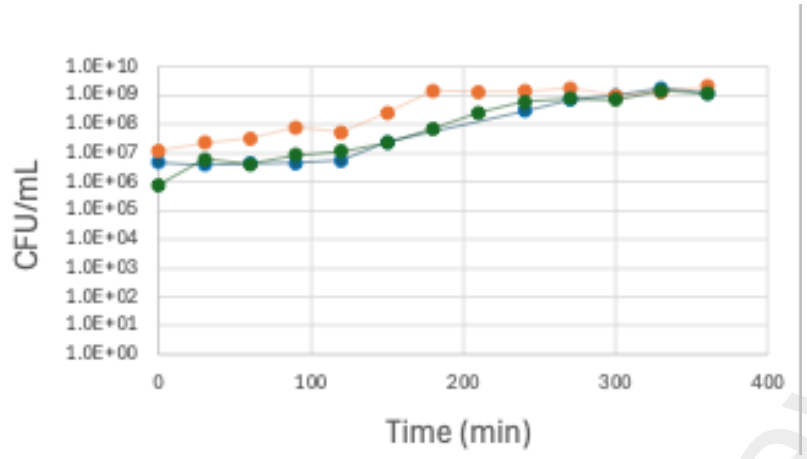

Figure S5: Colony forming units per mL (CFU mL^{-1}; logarithmic scale) and time for bacterial growth experiments (N=3).

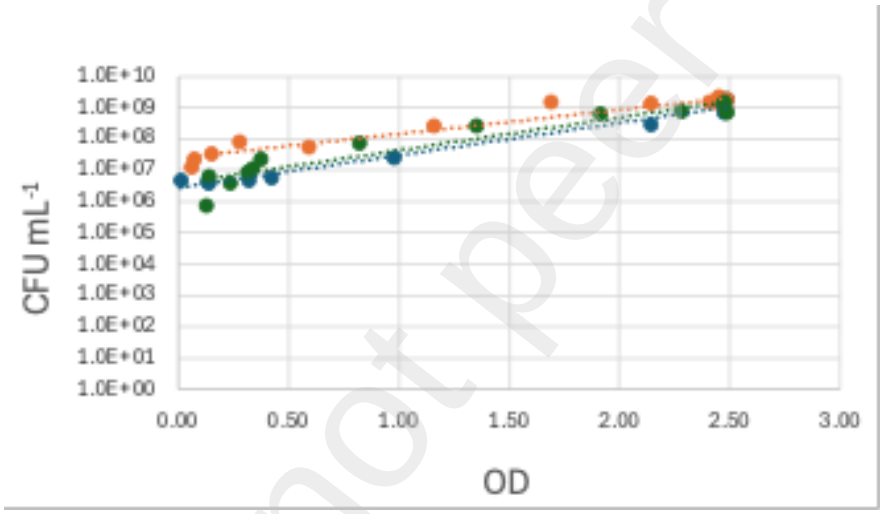

Figure S6: Colony forming units per mL (CFU mL^{-1}; logarithmic scale) and optical density (OD; wavelength=520 nm) for bacterial growth experiments (N=3).

When performing chamber experiments, we used the OD of the P-trap culture along with the relationship between CFU mL^{-1} and OD (see Figure S7) as a second method of quantification, to check that our plate count data is falling in the expected range and identify plate counts that may be vastly different, as a quality control check.

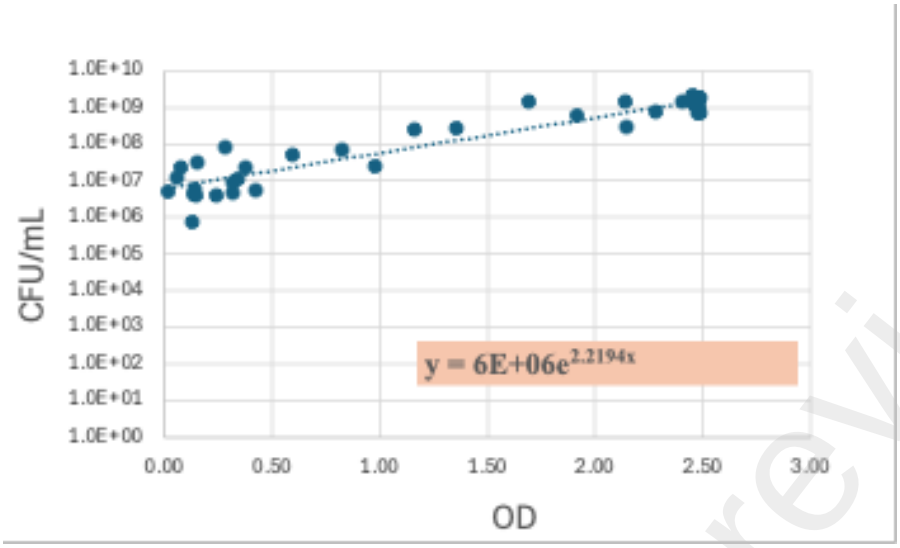

Figure S7: Colony forming units per mL (CFU mL^{-1}; logarithmic scale) and optical density (OD; wavelength = 520 nm) for bacterial growth experiments (N=3) plotted as one data set.

Section S4: Bioaerosol chamber experiments

Within 1-5 days prior to experiment, we prepared 50 culture plates for deposition as well as glass culture plates specific to the ACI using BD DIFCO™ MI Agar according to manufacturer instructions (See Table S6 for product details) (BD Diagnostics, 2025). We selected MI Agar for the chamber experiments to select for *E. coli* and minimize contamination from other sources. To prepare the aerosol chamber we first disinfected the P-trap in a bleach bath (1 L, 10% bleach), flushed the sink piping, and disinfected the inside of the sink bowl with bleach and ethanol. We grew the *E. coli* culture for the chamber experiments using the same growing procedures as the bacterial quantification experiments, (minus the plating and OD every 30 minutes). We removed one colony from a TSA plate streaked with E. *coli* F_{Amp} using a sterile inoculation loop and swirled it into 30 mL of tryptic soy broth (Table S6), then incubated it at 37°C with shaking (150 RPM) for 18 h. Following overnight incubation, 400 µL of culture was transferred to 120 mL of fresh TSB and incubated for an additional 6 hours. Note we increased

the total volume of the solution (from 90 mL to 120 mL) to fill the P-trap but kept the ratio consistent (100 µL culture / 30 mL of fresh TSB). Following the final 6-hour incubation we measured the optical density at 520 nm in triplicate and made serial dilutions of the culture up to 10^7 using PBS (Table S6), with the dilution factor expressed as a log reduction of the culture up to 10^7. We then plated the 10^5-10^7 dilutions in triplicate onto the freshly poured MI Agar plates (9 total) and left at room temperature until all plates were ready to be incubated. Our dilution plating counts will be our primary method of quantification, and we use the OD based estimation as a quality control check. The colony counts were a result of the average from the 9 dilution plate count results, while the OD-based CFU estimation was generated by plugging the culture OD into the equation in Figure S7, generated by the growth curve experiments.

Next, we placed a total of ten 100 mm x 15 mm agar plates on the sink counter and twenty plates on the chamber floor in predetermined and enumerated grid locations for consistent sampling (Figure S8). We installed the 6 glass MI Agar plates into the 6 stage Andersen Cascade Impactor and connected it to an external vacuum pump and a volumetric flowmeter (TSI, model 4046, Shoreview, MN) (Table S1). We placed the ACI inside the chamber on the sink counter with the tubing extending through chamber wall so that flow meter and vacuum pump were operable from outside the chamber. We ensured the HOBO and PurpleAir sensors had sufficient power and were logging data. Next, we introduced the 120 mL bacterial TSB culture into the empty sink P-trap in 30 mL increments using a sterile pipette. We placed the pipette tip through the metal strainer sink drain then slowly ejected, being careful not contaminate sink bowl or strainer with bacteria or cause splashing from P-trap. We removed all lids from deposition plates and sealed the chamber door. We set the fan voltage to 6.19 V (± 0.01) for 2.09 (± 0.05) air changes per hour. We let the chamber circulate HEPA filtered air for 30 min (1 air change) to

filter out any particles that may have been introduced while the chamber was open. While this occurred, we initiated the BioSpot "wet wicks" program according the manual to prepare it for sample collection. After wet wicks program finished, we placed 5 mL of 25 mM TRIS solution (the BioSpot sample deposition liquid) in a 35 mm x 11 mm petri dish and placed into BioSpot collection port. After HEPA filtered air had passed through the chamber for 30 min, we initiated BioSpot sample collection (8 L min^{-1}), setting the sample period to 32 minutes (including 2 minutes of buffer time while other instruments are set up). We then turned on ACI vacuum pump and adjusted the flow to 28.6 L min^{-1}. After the instruments were both sampling, we turned on the faucet to a water flow rate of 7.4 L min^{-1} (± 0.2) and the faucet let run for 3 continuous minutes before shutting it off. We let instruments continue to sample until 30 minutes had elapsed and the BioSpot had stopped automatically before turning off the ACI vacuum pump. We removed the petri dish from the BioSpot, measured the volume, and transferred the liquid sample to a sterile tube. We retrieved all ACI, counter and floor deposition plates from the chamber, and plated the entire BioSpot sample solution onto 3 MI agar plates. BioSpot samples are impacted into a liquid buffer of 5 mL, however depending on the hygroscopicity and concentration of the aerosol, as well as the ambient RH, the volume of liquid can decrease or increase to some extent during sampling. Thus, before BioSpot samples were plated, the remaining volume was measured and recorded to calculate the total CFU mL^{-1} of buffer solution. Plates consisted of those for: initial concentration estimation (9), counter deposition (10), floor deposition (20), BioSpot (3), and ACI (6). These plates were placed in the incubator at 37 °C for 20-24 h, according to MI Agar product instructions (BD Diagnostics, 2025). Following the incubation period, we removed and counted colonies on all plates.

We completed the dynamic blank experiment following the same methods but spiking 120 mL of tap water in the p-trap without the bacterial culture. The purpose of this negative control was to ensure that the source of our E. *coli* F_{Amp} CFUs was truly our culture and was not coming the tap water or residuals from previous experiments.

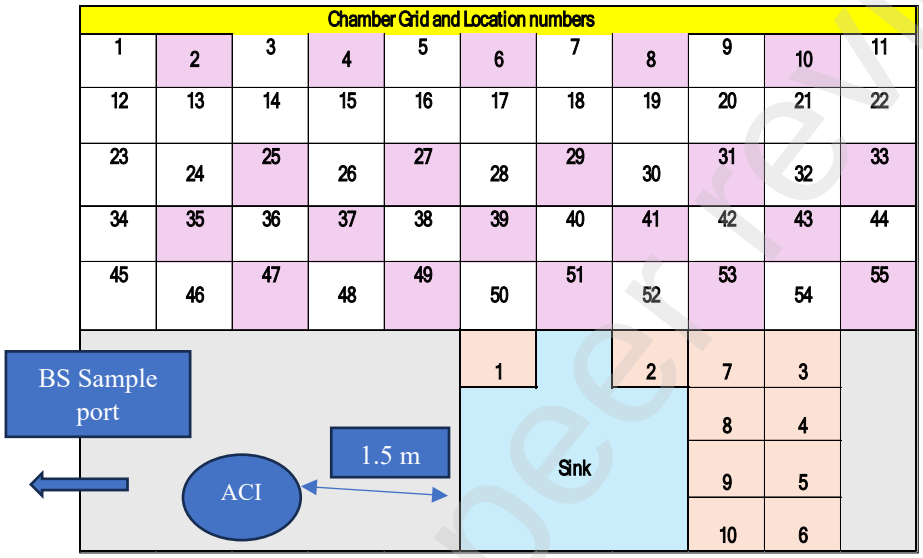

Figure S8: Spatial orientation of deposition plates: Squares highlighted pink indicate grid locations where deposition plates were placed. Squares highlighted orange annotate indicate counter plate locations. BioSpot (BS) was located outside the chamber, but the sampling tube ran through chamber wall (designated by arrow). Andersen Cascade Impactor (ACI) sampled from left side of sink at the same vertical height, and approximately 1.5 m horizontally from the sink. The vacuum tubing passed through the chamber wall so that pump and flow-meter could be operated from the chamber exterior.

Section S5. Additional experimental results

Table S7: Initial mean bacterial concentration estimates from triplicate culture of serial dilutions and optical density (OD) measurements for each chamber experiment. CFU counts from both methods are reported as well as the averages. Dilution plate counts are highlighted as they will be used in future calculations.

Experiment	Dilution plates (CFU mL^{-1})	OD (520 nm)	OD-based estimation (CFU mL^{-1})	Average (CFU mL^{-1})
Chamber 1	7.5×10^8	2.231	8.5×10^8	7.9×10^8
Chamber 2	8.9×10^8	2.348	9.3×10^8	9.1×10^8
Chamber 3	1.1×10^9	2.349	1.1×10^9	1.1×10^9
Chamber 4	3.4×10^9	2.335	1.1×10^9	2.3×10^9
Chamber 5	6.6×10^8	2.302	9.9×10^8	8.3×10^8
Average	1.4×10^9	2.313	9.9×10^8	1.2×10^9

Table S8: CFU totals by grid location and experiment number for floor-placed deposition plates. Floor plate location refers to grid square numbers associated with location on chamber floor.

Floor Plate Location	13-Feb	19-Feb	20-Feb	27-Feb	28-Feb	BLANK	Total CFU
2	1	0	0	0	0	0	1
4	0	7	0	3	0	0	10
6	0	0	0	0	0	0	0
8	1	0	0	0	0	0	1
10	0	0	0	0	0	0	0
25	5	0	0	0	0	0	5
27	0	0	0	0	0	0	0
29	2	0	0	0	0	0	2
31	1	0	0	0	0	0	1
33	3	0	0	0	0	0	3
35	1	0	0	0	0	0	1
37	0	0	0	0	0	0	0
39	0	3	0	0	0	0	3
41	1	2	0	0	0	0	3
43	2	2	0	0	0	0	4
47	1	0	0	1	0	0	2
49	0	0	1	0	1	0	2
51	0	15	0	0	0	0	15
53	1	1	0	2	2	0	6
55	0	0	0	5	0	0	5
Total	**19**	**30**	**1**	**11**	**3**	**0**	**64**

Table S9: CFU totals by grid location and experiment number for counter-placed deposition plates. Counter location refers to grid square numbers associated with location in chamber (Figure S8).

Counter Location	13-Feb	19-Feb	20-Feb	27-Feb	28-Feb	BLANK	Total CFU
1	1	3	14	3	2	0	23
2	4	2	0	14	6	0	26
3	0	27	0	0	1	0	28
4	3	0	0	0	0	0	3
5	1	6	0	3	0	0	10
6	3	0	0	9	0	0	12
7	1	1	17	0	0	0	19
8	2	0	0	1	1	0	4
9	0	0	6	29	0	0	35
10	4	5	5	0	0	0	14
Total	**19**	**44**	**42**	**59**	**10**	**0**	**174**

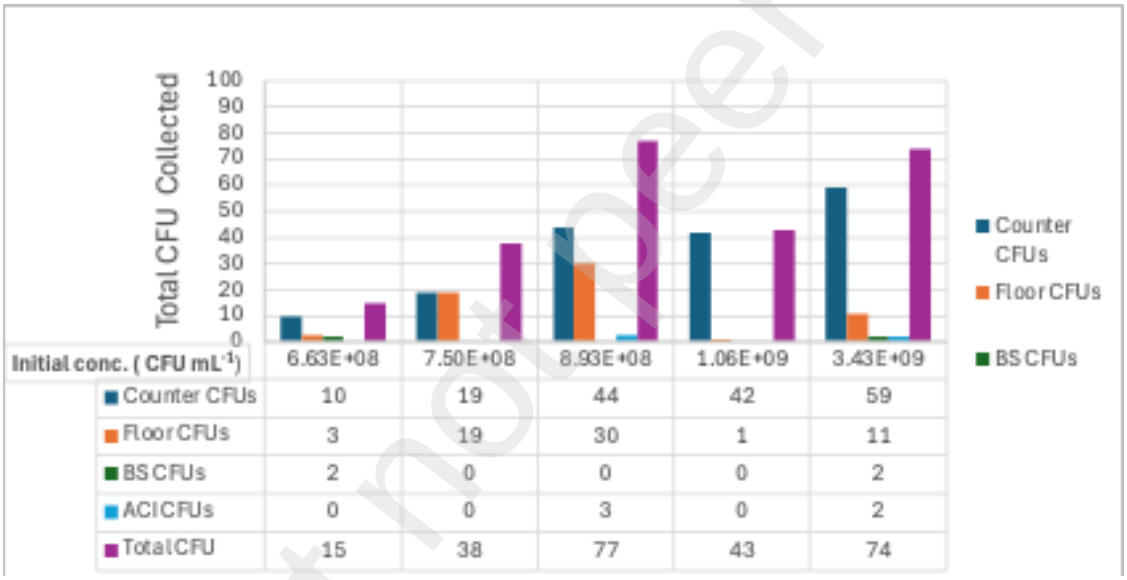

Initial conc. (CFU mL^{-1})	6.63E+08	7.50E+08	8.93E+08	1.06E+09	3.43E+09
Counter CFUs	10	19	44	42	59
Floor CFUs	3	19	30	1	11
BS CFUs	2	0	0	0	2
ACI CFUs	0	0	3	0	2
Total CFU	15	38	77	43	74

Figure S9: Total CFUs collected by sample type across 5 experiments by initial concentration of *E. coli* inoculant spiked in sink drain.

Section S6. Risk assessment calculation methods and supplemental results

To assess the risk of patient contact from sink-generated bioaerosol in the hospital setting, we first estimated the room averaged bacterial concentration immediately after 3 min of sink operation (0.39 and 0.56 CFU m^{-3}) in a room with *K. pneumoniae* colonization (1.4 x 10^{9} CFU mL^{-1} in a p-trap with 120 mL of water) using the lower bound and upper bound air emission

factors reported in Table 4 (1.3 x 10^{-10} and 1.9 x 10^{-10} CFU emitted per CFU spiked, respectively) and a room volume of 56.63 m^3 as shown in Equation S4 for the lower bound EF:

$$bacterial\ conc.\ in\ air\left(\frac{CFU}{m^3}\right) = \frac{1.4x10^9\left(\frac{cfu}{mL}\right) * 120\ mL * 1.3\ x10^{-10}\left(\frac{CFU}{CFU}\right)}{56.63\ m^3} = 0.39\ \left(\frac{CFU}{m^3}\right) \quad \text{(S4)}$$

Over the course of the hour before the sink is operated again, concentrations decrease with time due to air exchange (Equation 5) as shown for the lower bound EF in Equation S5 and Figure S10, where time is given in hours and concentration in CFU m^{-3}:

$$C(t) = 0.39 * e^{-6(t)} \quad \text{(S5)}$$

Next, we estimated the dose (Equation 6) inhaled by a patient over the course of the hour after the sink was operated to be 0.0324 and 0.0466 CFU and using the initial hourly air concentrations (0.39 and 0.56 CFU m^{-3}, respectively) and decay as shown above. According to the EPA, the average adult at rest inhales 0.5 m^3 of air per hour (U.S. Environmental Protection Agency, 2011). This is illustrated in Equation S6 for an initial concentration of 0.39 CFU m^{-3}:

$$Total\ CFUs\ inhaled = 0.5\ m^3 \int_0^{1.0} C(t)dt = (.5\ m^3)\int_0^{1.0} C_0 * e^{(-\lambda)t}\ dt$$

$$= (0.5\ \frac{m^3}{h}) * (0.39\ \frac{CFU}{m^3}) * (\frac{1}{6}\ h)(1 - e^{-6*(1.0)}) = 0.032\ CFU \quad \text{(S6)}$$

where λ is the ACR at 6 h^{-1}, inhalation rate is 0.5 m^3 h^{-1}, time (t) is in hours, and $C(t)$ is concentration in CFU m^{-3}.

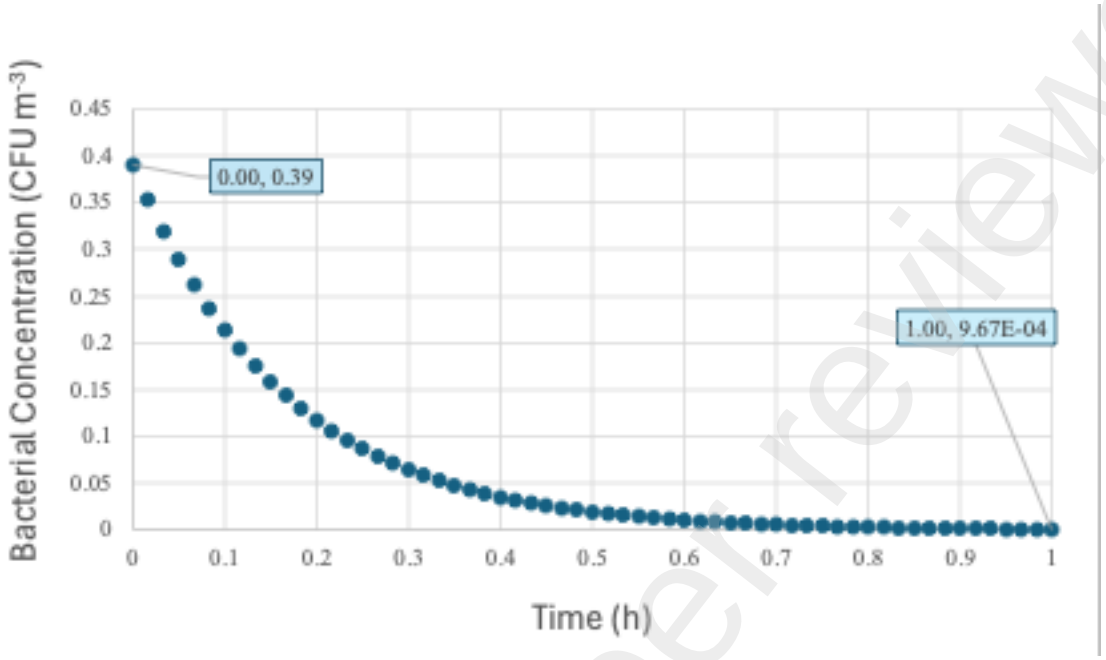

Figure S10: Estimated average hospital room bioaerosol concentration over the hour after sink operation, given a room size of 56.36 m^3 and an ACR of 6 h^{-1}. Data labels highlight concentrations at t=0 and t=1 h.

Over 24 hours, assuming the sink is operated once per hour, this results in a dose of 0.778 and 1.12 CFU per day, applying the lower bound and upper bound bioaerosol emission factors, respectively. Next, we applied the dose inhaled to the dose response model with *k* of 1.62 x 10^{-6} for *K. pneumoniae* (Denissen et al., 2022), as illustrated in Equation S7 for the lower bound EF:

$$P_{inf} = 1 - e^{-(0.78)*(1.62\ x\ 10^{-6})} \quad \text{(S7)}$$

We estimated the probability of infection over 24 hours to be 1.3 x 10^{-6} to 1.8 x 10^{-6} based on lower to upper bound bioaerosol EFs, respectively. Probability of infection for a 5.5 day and one year hospital stay were also calculated as described in the main text. A sensitivity analysis with a

factor of ten smaller P-trap concentration was also performed using the methods described above.

Section S7. Aerosol number concentrations

Over the 5 experiments and 1 control, real-time $PM_{5.0}$ number concentrations (number concentration of particles smaller than 5.0 μm in diameter) from the PurpleAir ranged from 3.50 x 10^3 - 4.77 x 10^5 m^{-3}, and the number concentrations of particles greater than 5 μm in diameter ranged from 8.00 x 10^2 - 2.09 x 10^3 m^{-3}. Typical indoor air particle number concentrations vary greatly. Previous literature has reported particle number concentrations from 500 m^{-3} (HEPA filtered air, particles 0.3 μm - 20 μm in diameter), to 1.65 x 10^9 m^{-3} (particles 0.1 μm - 0.53 μm in diameter), to as high as 1.5 x 10^{10} m^{-3} (particles < 2.5 μm in diameter). Our particle number concentrations fall within the lower end of that range (Hussein et al., 2006, 2019; Morawska et al., 2009). Although concentration vary across and between experiments, particle number concentrations do not show clear increases corresponding to periods of sink operation, implying that bioaerosol generated during sink use had a negligible impact on total particle number concentrations for both particles less than and greater than 5.0 μm in diameter.

Section S8. Particle losses

To examine the scale of $PM_{5.0}$ wall losses in the chamber, we added particle deposition to the mass balance equation and considered the measured decrease in the PurpleAir $PM_{5.0}$ particle number concentration as room air is replaced with HEPA filtered air in the chamber. We

$$-\ln\left(\frac{P(t) - P_{baseline}}{P_0 - P_{baseline}}\right) = (\lambda + k')t \quad \text{(S8)}$$

compared this decrease to what is expected for based on air change rate alone. For this purpose, the mass balance equation is rearranged to give (Equation S8):

where $P(t)$ is particle number concentration as a function of time t (m^{-3}); λ is air change rate (h^{-1}); k' is particle deposition (wall loss) rate (h^{-1}); $P_{baseline}$ is the baseline/minimum particle counts; P_0 is the initial particle number concentration (m^{-3}), and t is time (h^{-1}). To apply this equation, we opened the chamber to introduce particles, then let it remain open overnight before sealing the chamber for particle removal. The fan voltage was set to 6.19 (±.01) V, corresponding to an air change rate of 2 h^{-1}. PurpleAir particle number concentration data from those periods of time are shown in Figure S11. In Figure S12, we show the natural log of the measurements vs time so that the slope is an expression of $\lambda + k'$ (Equation S8). The slope from the 3 particle decay experiments ($\lambda + k' = 2.01 \pm 0.07$ h^{-1}; Figure S12) is comparable to the chamber air change rate ($\lambda = 2.01 \pm 0.05$ h^{-1}), suggesting that particle wall losses are small. This is consistent with expectations, since we expect losses for 5 μm diameter aerosol particles to be <15% based on

their terminal settling velocity (Hinds and Zhu, 2022). However, it is important to note that this does not consider losses of larger particles and droplets to the chamber walls and floor.

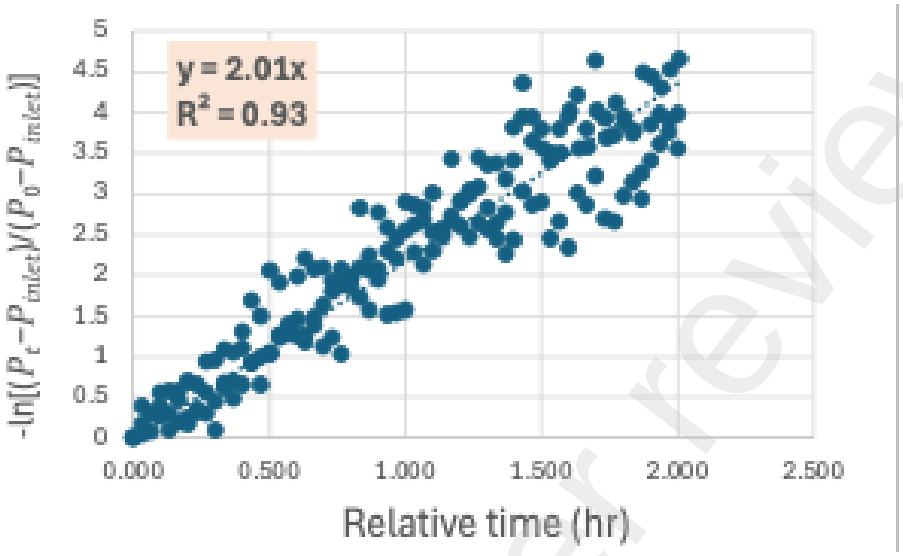

Figure S12: The particle decay rate over 2 hours for 3 particle decay experiments.

Section S9. References

BD Diagnostics. (2025). *Difco™ & BBL™ Manual: MI Agar* (No. Section III-M; Difco™ & BBL™ Manual). Becton, Dickinson and Company.

Denissen, J., Reyneke, B., Waso-Reyneke, M., Havenga, B., Barnard, T., Khan, S. and Khan, W. (2022). Prevalence of ESKAPE pathogens in the environment: Antibiotic resistance status, community-acquired infection and risk to human health. *International Journal of Hygiene and Environmental Health*, *244*, 114006.

Hinds, William C., and Yifang Zhu. *Aerosol technology: properties, behavior, and measurement of airborne particles*. John Wiley & Sons, 2022.

Hussein, T., Alameer, A., Jaghbeir, O., Albeitshaweesh, K., Malkawi, M., Boor, B. E., Koivisto, A. J., Löndahl, J., Alrifai, O., & Al-Hunaiti, A. (2019). Indoor Particle Concentrations, Size Distributions, and Exposures in Middle Eastern Microenvironments. Atmosphere, 11(1), 41. https://doi.org/10.3390/atmos11010041

Hussein, T., Glytsos, T., Ondráček, J., Dohányosová, P., Ždímal, V., Hämeri, K., Lazaridis, M., Smolík, J., & Kulmala, M. (2006). Particle size characterization and emission rates during indoor

activities in a house. Atmospheric Environment, 40(23), 4285–4307. https://doi.org/10.1016/j.atmosenv.2006.03.053

Morawska, L., Johnson, G. R., Ristovski, Z. D., Hargreaves, M., Mengersen, K., Corbett, S., Chao, C. Y. H., Li, Y., & Katoshevski, D. (2009). Size distribution and sites of origin of droplets expelled from the human respiratory tract during expiratory activities. Journal of Aerosol Science, 40(3), 256–269. https://doi.org/10.1016/j.jaerosci.2008.11.002